ACS SyntheticBiology

Research Article

pubs.acs.org/synthbio

Molecular Titration Promotes Oscillations and Bistability in Minimal Network Models with Monomeric Regulators

Christian Cuba Samaniego,[†] Giulia Giordano,[‡] Jongmin Kim,[¶] Franco Blanchini,[‡] and Elisa Franco*[,†]

[†]Mechanical Engineering, University of California at Riverside, Riverside, California 92521, United States

[‡]Mathematics and Computer Science, University of Udine, 33100 Udine, Italy

[¶]Wyss Institute for Biologically Inspired Engineering, Harvard University, 3 Blackfan Circle, Boston, Massachusetts 02115, United States

Supporting Information

ABSTRACT: Molecular titration is emerging as an important biochemical interaction mechanism within synthetic devices built with nucleic acids and the CRISPR/Cas system. We show that molecular titration in the context of feedback circuits is a suitable mechanism to enhance the emergence of oscillations and bistable behaviors. We consider biomolecular modules that can be inhibited or activated by input monomeric regulators; the regulators compete with constitutive titrating species to determine the activity of their target. By tuning the titration rate and the concentration of titrating species, it is possible to modulate the delay and convergence speed of the transient response, and the steepness and dead zone of the stationary response of the modules. These phenomena favor the occurrence of oscillations when modules are interconnected to create a negative feedback loop; bistability is favored in a positive feedback interconnection. Numerical simulations are supported by mathematical analysis showing that the capacity of the closed loop systems to exhibit oscillations or bistability is structural.

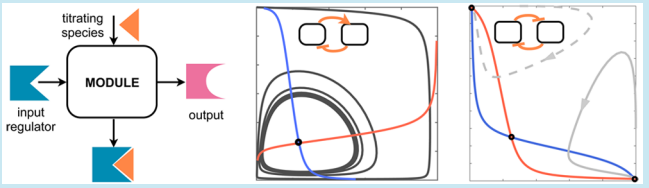

KEYWORDS: *titration, oscillations, bistability, monomeric regulator, delays, synthetic biology, RNA*

The construction of complex dynamic circuits from programmable parts, with behaviors that are predictable and easy to engineer, has been one of the overarching goals of synthetic biology since its early steps.[1−3] The pool of available parts has been largely expanded with the development of RNA-based devices, such as riboregulators and siRNA, which are becoming increasingly popular due to the rapid programmability of RNA secondary structure and function.[4−8] Recently, the CRISPR/Cas system (which relies on guide RNA molecules) has revolutionized existing methods for synthetic control of gene expression,[9,10] and promises to enable the creation of virtually arbitrary regulatory interactions.

These rapidly evolving RNA nanotechnologies present a unique challenge in the context of building complex dynamic circuits: RNA-based regulatory interactions are noncooperative in general, meaning that one copy of RNA-driven regulator binds to its target site, rather than forming multimers like many transcription factors. Cooperativity is well-known for yielding sharp dose responses with tunable thresholds,[11] which are nonlinearities generally required (within a feedback circuit) to obtain oscillations and multistationarity. An alternative to cooperativity is the mechanism of molecular titration,[12,13] present in many natural examples of protein sequestration in signaling pathways,[14,15] which can generate tunable ultrasensitive responses using stoichiometric interactions between monomers. Titration can also generate delays, which are known to promote oscillations.[16,17] Thus, molecular titration is an ideal candidate mechanism to build dynamic circuits using monomeric regulators.

In this article we show that biomolecular processes driven by monomeric regulators can be combined to obtain oscillations and bistability. We consider minimal systems whose output can be repressed or activated by an increase in input monomers. These monomers bind to and control the production rate of a target molecule that represents the module output; the monomer input can be titrated by competing species that serve as constitutive activators or inhibitors. By modulating the parameters of the titration process we can control the steady state and the temporal response of the modules. In particular, we show that the total concentration of titrating species modulates the steady-state response threshold (or "dead-zone") and the delay in the temporal response; the titration reaction rate influences the steepness of the on/off transitions in the steady state and transient response.

We interconnect modules to form canonical signal generators in biomolecular systems. Oscillators are important in biological organisms because they drive and synchronize the activity of downstream pathways.[18] Timing signals are needed for synthetic molecular systems as well, and many artificial oscillators have been built *in vivo*[1,16,19−22] and *in vitro*.[23−25] Bistable systems are equally relevant as they achieve robust on−

Received: September 20, 2015
Published: January 21, 2016

DOI: 10.1021/acssynbio.5b00176
ACS Synth. Biol. 2016, 5, 321−333

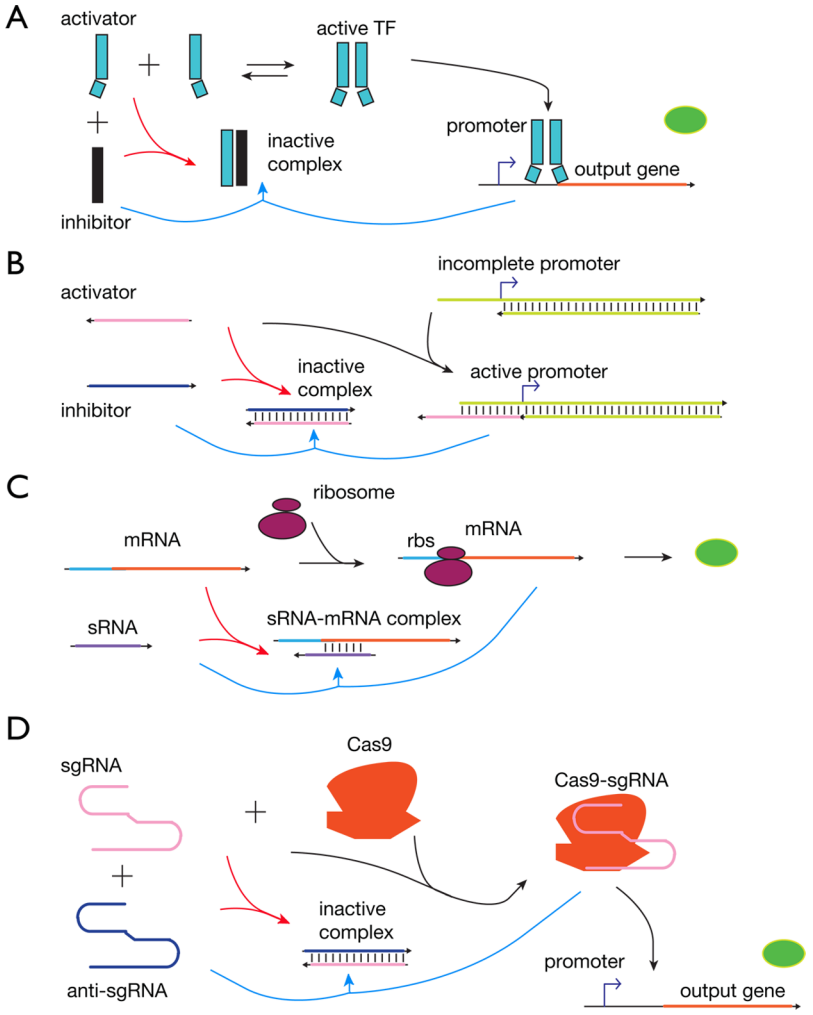

Figure 1. Examples of natural and synthetic gene expression regulatory pathways where monomeric molecules determine the activity of a target (indirect titration, blue reaction arrows) and can be annihilated by competing species (direct titration, red reaction arrows). (A) Monomeric transcription factor titrated by an inhibitor.[13] (B) Synthetic DNA activators binding to the promoter region of linear templates can be titrated out by complementary DNA or RNA inhibitors.[28] (C) mRNA and ribosome binding can be prevented by sRNA molecules which titrate the mRNA.[35] (D) Guide RNA and Cas9 bind to form the active Cas9-sgRNA complex;[36] sgRNA is titrated by an anti-sgRNA molecule forming an inactive complex.

off behaviors and serve as memory elements in signal transduction and developmental networks,[26,27] as well as being important components in artificial systems.[2,19,28,29]

Our approach combines numerical simulations and rigorous mathematical analysis. The models we consider have many parameters, and it is desirable to establish what their admissible dynamic behaviors are in a wide range of parameter variability, or—ideally—for arbitrary parameter choices. We employ control and dynamical systems methods and identify stability and monotonicity[27,30] properties of the inhibited and activated modules; we say that these properties are structural because they do not depend on the specific parameters chosen.[31] When these modules are interconnected to form a negative or a positive feedback loop, we can conclude that they can exclusively admit instability of oscillatory or bistable nature (respectively). These results are consistent with the famous Thomas' conjectures.[32−34] Simulations are required to identify parameter values yielding the desired dynamics: we numerically integrate the models of the candidate dynamic networks and study the parameter range in which the desired behavior is achieved. The combination of theoretical analysis and simulations reveals that direct titration is not necessary to achieve oscillations and bistability, but it significantly promotes their occurrence.

Our analysis points out design principles that render molecular titration amenable to building a variety of feedback circuits using monomeric regulators. For instance, gene networks can be regulated via protein titration, as pioneered by Buchler and colleagues (Figure 1A).[12,13] Our results are particularly relevant to nucleic acid systems, because nucleic acids are naturally amenable to designing competitive binding and titration reactions to elicit nonlinear responses. Several synthetic *in vitro* circuits including bistable circuits and oscillators were constructed utilizing molecular titration reactions (Figure 1B).[23,28] Indeed, natural examples of titration-based RNA regulatory parts abound, including sequestration of mRNA by sRNA to regulate translation and mRNA degradation (Figure 1C)[35] — these features can contribute to robust multiple target gene regulation and threshold responses.[37] Synthetic biological circuits in the future will benefit from the targeting specificity and broad utility of CRISPR/Cas system.[36] Nuclease mutant Cas9 proved to be useful in constructing synthetic logic circuits by utilizing simple design change of guide RNA sequences to target desired DNA

DOI: 10.1021/acssynbio.5b00176
ACS Synth. Biol. 2016, 5, 321−333

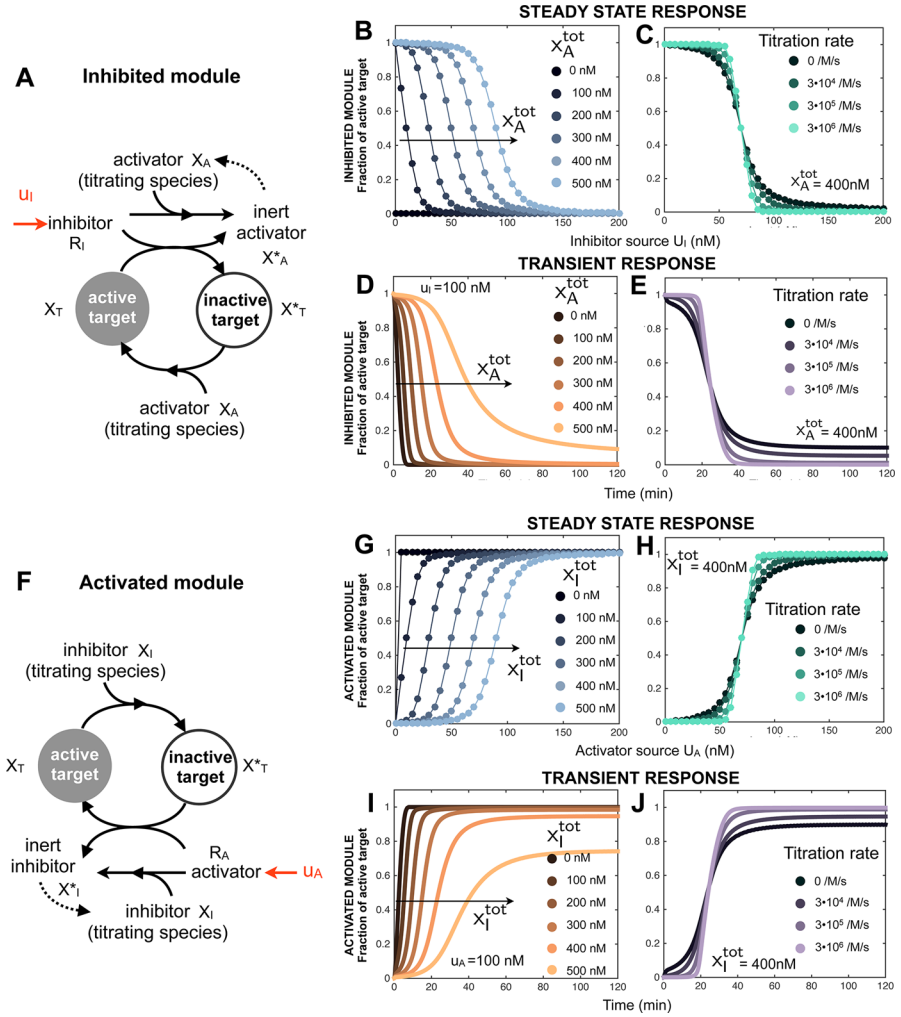

Figure 2. Stationary and transient behavior of the inhibited and activated modules described in the Minimal inhibited and activated modules section. (A) Scheme of the inhibited module. (B) Steady state fraction of target X_T as a function of the input u_I (source of inhibitor R_I), for varying amounts of total constitutive activator X_A. By increasing x_A^{tot}, we move the "dead zone" of the response to the right. (C) Steady state fraction of active target as the titration rate ν varies, for x_A^{tot} = 400 nM; a large titration rate corresponds to a sharper on−off transition. (D) Transient response of the active fraction of x_T for varying amounts of x_A^{tot}; large x_A^{tot} introduces a delay in the time it takes for the system to reach steady state. (E) The transient response of the inhibited module (active fraction of x_T) shows a sharper transition for large titration rate ν. (F) Scheme of the activated module. (G) Steady state fraction of target x_T as a function of u_A, for varying amounts of x_I^{tot}. (H) Steady state response of the activated module, with increasing titration rate ν, and x_I^{tot} = 400 nM. (I) Transient response of the active fraction of x_T in the activated module as a function of x_I^{tot}, showing how delay is increased. (J) Transient response of the activated module (active fraction of x_T); the transition is sharper as the titration rate ν increases.

sequence domains for repression and activation. Still, lack of ultrasensitive response proved challenging when layering gates.[9,10] It is likely that an analogous approach utilizing molecular titration can yield ultrasensitivity in CRISPR/Cas system and allow fine-tuning of circuit dynamics (Figure 1D).

RESULTS

Minimal inhibited and activated modules. We consider molecular modules where monomeric activators and inhibitors compete to determine the fraction of a target that is in an active (X_T) or inactive (X_T^*) state. We say that our models are minimal because activators and repressors are monomeric, and regulatory reactions are solely uni- and bimolecular. In the rest of this article we indicate a chemical species with an uppercase letter, and its concentration with the corresponding lowercase letter (e.g., species A has concentration a).

An inhibited module is composed of the target X_T, a constitutive activator X_A, and is regulated by the inhibiting species R_I (Figure 2A). Similarly, an activated module is composed of the target X_T, a constitutive inhibitor X_I, and an activator R_A (Figure 2F). We assume that the total concentration of target is constant: $x_T + x_T^* = x_T^{tot}$ at any point in time. This assumption is reasonable if the target is, for instance, a gene whose copy number is constant. Similarly, we assume that the total concentration of constitutive inhibitor and constitutive activator are constant in each module; in other words, we assume that the time scale of their production and degradation is much slower than the regulatory reactions within the modules, and can thus be neglected for the purpose of our analysis. Like the target X_T, the constitutive inhibitor X_I and activator X_A switch between a functional and inert state while their total concentrations remain constant. This assumption is handy because it allows us to examine the behavior of each system treating the total concentration of constitutive activator/inhibitor species as a design parameter. The inert constitutive activators/inhibitors are converted back to their

DOI: 10.1021/acssynbio.5b00176
ACS Synth. Biol. 2016, 5, 321−333

active form at a constant rate. Finally, we assume that the activators and inhibitors R_A and R_I are produced by "input" species U_A and U_I respectively, and are degraded at a constant rate.

The regulators R_I and R_A bind directly to their target X_T and X_T^* controlling the amount of its active fraction. In addition, regulators can bind to the constitutive inhibitor or activator: these interactions result in titration of the regulators available for direct target binding. We will focus on the inhbited regulator in more detail. Inhibitor R_I binds to active target X_T ($X_T^*{\cdot}X_A$ complex), converting it to inactive target X_T^* and releasing inert constitutive activator X_A^* ($X_A{\cdot}R_I$ complex); R_I is sequestered in this inactive complex; X_A^* spontaneously recovers its activity over time through degradation of R_I in the complex. R_I also binds to free X_A, yielding the inert complex X_A^* ($X_A{\cdot}R_I$ complex where R_I is sequestered). A large amount of free X_A in solution can thus titrate R_I, delaying inhibition of the target. R_I is also degraded at a constant rate. The activated module works in a similar manner.

The reactions modeling the release of X_A and X_I as inert species, and their subsequent recovery, are consistent with our assumption that the total concentration of X_A/X_I remains constant (molecules of X_A/X_I are not produced nor degraded, they only switch between active and inert form). In addition, these reactions model very well the toehold-mediated branch migration processes in nucleic acid transcriptional circuits.[28,38] In this case, R_I is an RNA species displacing a portion of the promoter X_A from a synthetic gene X_T.[23,24,28] X_A displaced from X_T ($X_T^*{\cdot}X_A$ complex) by R_I forms an inert complex X_A^* ($X_A{\cdot}R_I$ complex); RNase H degradation of R_I bound to X_A results in recovery of X_A. In general, X_I and X_A could be proteins or RNA species designed to bind to and titrate the input regulators R_A and R_I respectively.[39,40] We refer to these reactions as "direct titration" or simply titration. The reactions between regulators R_I and R_A, and the complexes X_A and X_I bound to targets X_T^* and X_T, indicated as "inhibition" and "activation" reactions respectively, can be classified as titration reactions as well, but in this context we refer to them as "indirect titration". Molecular titration is a well-known mechanism to generate ultrasensitivity and delays[12,13] (Figure 1A); we will describe how these properties can be achieved and tuned by controlling the direct titration reaction.

The reactions defining each module are listed below. (For simplicity we denote reaction rates with the same symbols when they have the same function in the two modules.)

	Inhibited module		Activated module
Constitutive activation:	$X_T^* + X_A \xrightarrow{\alpha} X_T$	Constitutive inhibition:	$X_T + X_I \xrightarrow{\delta} X_T^*$
Inhibitor production:	$U_I \xrightarrow{\beta} U_I + R_I$	Activator production:	$U_A \xrightarrow{\beta} U_A + R_A$
Inhibition:	$X_T + R_I \xrightarrow{\delta} X_T^* + X_A^*$	Activation:	$X_T^* + R_A \xrightarrow{\alpha} X_T + X_I^*$
Direct titration:	$X_A + R_I \xrightarrow{\nu} X_A^*$	Direct titration:	$X_I + R_A \xrightarrow{\nu} X_I^*$
Recovery:	$X_A^* \xrightarrow{\kappa} X_A$	Recovery:	$X_I^* \xrightarrow{\kappa} X_I$
Degradation:	$R_I \xrightarrow{\phi} \emptyset$	Degradation:	$R_A \xrightarrow{\phi} \emptyset$

Because the total concentration of species X_T, X_I, and X_A is constant, we can write the following mass conservation equalities: $x_T^{tot} = x_T + x_T^*$, $x_I^{tot} = x_I + x_I^* + x_T^*$, and $x_A^{tot} = x_A + x_A^* + x_T$. Figure 2A and F show a graphical representation of the two modules and their reactions. Using the law of mass action and the mass conservation equalities, we obtain the following model for the inhibited module:

$$\dot{x}_T = \alpha(x_T^{tot} - x_T)x_A - \delta x_T r_I \quad (1)$$

$$\dot{x}_A = \kappa(x_A^{tot} - x_A - x_T) - \alpha(x_T^{tot} - x_T)x_A - \boxed{\nu x_A r_I} \quad (2)$$

$$\dot{r}_I = \beta u_I - \phi r_I - \delta x_T r_I - \boxed{\nu x_A r_I}. \quad (3)$$

The differential equations describing the activated module are

$$\dot{x}_T = \alpha(x_T^{tot} - x_T)r_A - \delta x_T x_I \quad (4)$$

$$\dot{x}_I = \kappa(x_I^{tot} - x_I - (x_T^{tot} - x_T)) - \delta x_T x_I - \boxed{\nu x_I r_A} \quad (5)$$

$$\dot{r}_A = \beta u_A - \phi r_A - \alpha(x_T^{tot} - x_T)r_A - \boxed{\nu x_I r_A}. \quad (6)$$

Boxes highlight terms associated with the titration reactions between constitutive activators/inhibitors and the input regulators. Before exploring numerically the behavior of these differential equations, we point out some important properties of the stationary and transient behavior of these systems.

Structural properties. The concentration of each species in the modules is bounded for arbitrary (positive and bounded) values of the binding rates, and of initial and total concentration of the species. By assumption, the total concentration of the target X_T and the total concentration of the constitutive activator X_A and inhibitor X_I are constant, thus $x_T(t) \le x_T^{tot}$, $x_A(t) \le x_A^{tot}$ and $x_I(t) \le x_I^{tot}$ at any time. As for the regulator inputs, the presence of a first order degradation rate ensures that their concentrations are bounded. For the inhibited subsystem, for instance, note that $\dot{r}_I(t) \le \beta u_I^{max} - \phi r_I$. By applying the comparison principle, we conclude that $r_I(t) \le r_I(0)\, e^{-\phi t} + u_I^{max}\beta(1-e^{-\phi t})/\phi$, which ensures $r_I(t) \le \max\{r_I(0), u_I^{max}\beta/\phi\}$ at any point in time; see Propositions 3 and 9, Supporting Information (SI) Section 1.

Expressions that relate the steady state of the active target concentration x_T to the concentration of the species producing regulators are derived in Section 1 of the SI. In the absence of titration reactions it can be shown analytically that the steady state curves that relate the input regulator source concentrations to the active target concentration are monotonic curves: the steady state mapping of the inhibited module $x_T = g(u_I)$ is decreasing; the steady state mapping of the activated module $x_T = k(u_A)$ is increasing (Propositions 1 and 7, SI, Section 1). Due to the monotonicity of the equilibrium curves, equilibria are unique once u_I or u_A are fixed. In the presence of titration reactions, numerical simulations indicate that monotonicity is preserved in the parameter range we considered (see Figure 2B, C, G, H). Monotonicity of the steady state input/output relationships is important to identify admissible equilibria in *interconnections* of modules, which will be considered in the following sections.

The behavior of these systems around the equilibrium point can be examined by linearizing the differential equations. In the absence of titration reactions, the Jacobian matrices of the inhibited and activated modules show that both systems are monotone. This property is satisfied if the total concentration of constitutive activator x_A^{tot} and inhibitor x_I^{tot} is larger than the concentration of target x_T^{tot}; it is also required that the difference $(x_A^{tot} - x_T^{tot})$ be larger than ratio of the recovery to activation rate κ/α; similarly we require that $(x_I^{tot} - x_T^{tot}) \ge \kappa/\delta$. If these assumptions are satisfied, then the Jacobian of each module is a sign definite Metzler matrix, which means that both modules are input/output monotone for arbitrary choices of the remaining parameters (details are provided in the SI, Section

DOI: 10.1021/acssynbio.5b00176
ACS Synth. Biol. 2016, 5, 321−333

1, Propositions 4 and 10). Uniqueness of the equilibria and monotonicity allow us to conclude that, in the absence of titration, both modules are *stable* (Propositions 4 and 10, SI, Section 1): for arbitrary values of the parameters, the systems always reach a stable fixed point (for any constant input value).

In the presence of titration reactions, boundedness and stability are preserved (see SI, Section 1), however monotonicity is only guaranteed when the equilibrium values of x_A and x_I are sufficiently large; this condition can be likely satisfied by increasing their total concentrations.

Boundedness of the solutions, monotonicity of the equilibrium input/output maps, monotonicity of the linearized dynamics, and stability are all important properties when considering these modules in the context of larger circuits.[31,41] The fact that these properties hold for (nearly) arbitrary choices of parameters indicates that our minimal systems may be treated as input/output modules. These modules can be interconnected creating predictable, robust feedback loops whose net positive or negative sign does not depend on the parameters.

The concentration of titrating species modulates the dose response threshold and the delay of the time response. Using the parameters reported in Table 1, we numerically solved the differential equations describing the inhibited and the activated modules, examining their steady state (Figure 2B, C, G, H) and their transient response (Figure 2D, E, I, and J). The steady state fraction of active target x_T/x_T^{tot} shows a Hill-type dose response to the concentration of species U_A or U_I that produce the regulator; the response threshold can be increased by increasing the total concentration of constitutive activator or inhibitor (titrating species). For example, Figure 2B shows that the steady state fraction of active target decreases as the concentration of U_I (the species producing inhibitor) increases; as the concentration of constitutive activator (titrating species) is increased up to 500 nM, the inhibition threshold moves to the right reaching about 100 nM. A similar behavior is observed for the activated module in Figure 2G. The dynamical effect of an increase in titrating species concentration is a temporal delay in reaching steady state, as shown in Figure 2D and I; for the reaction rates chosen in this example, the delay can reach 25−30 min. We numerically explored the role of the titration reaction rate, whereby constitutive activators and inhibitors sequester available regulator input. While the titration reactions are not required to obtain the qualitative threshold-dependent dose response and the time delay, their presence sharpens both responses. As shown in Figure 2C and H, the larger the titration rate the sharper is the transition between on and off states at steady state, once a certain U_I or U_A input threshold is reached. Figure 2E and J show that the temporal switch between fully on and fully off states of the target becomes sharper as the titration rate increases. We remark that in the absence of titration ($\nu = 0$) the systems still exhibit a dose response threshold and a delay in the time response; large values of ν yield sharper nonlinear behaviors, in particular increased ultrasensitivity and faster temporal switch in activity. Parameter sensitivities for the inhibited and activated modules are further explored in Figures S1 and S2.

To characterize the dynamic response of the modules we integrated the differential equations varying the signal source, target and titrating species concentration. As a measure of the delay, we then quantified the rise time of the target response, defined as the time it takes for the target concentration to reach 60% of its steady state value. Results are shown in Figure 3: the rise time is most dramatically influenced by the concentration of titrating species, and increases proportionally to it; as expected, the rise time is reduced by increasing the concentration of source signal.

Table 1. Parameters for the Inhibited System (Eqs 1−3) and for the Activated System (Eqs 4−6)

Rate	Description	Value	Other studies
α (/M/s)	Activation	3×10^5	
δ (/M/s)	Inhibition	3×10^5	Nucleic acids: 10^4−10^6, refs 28, 42
ν (/M/s)	Titration rate	3×10^5	Protein/Protein: 10^4−10^6, refs 43, 44
β (/s)	Production of regulator	5×10^{-3}	RNA: 10^{-3} to 1, refs 45, 46
			Proteins: 3×10^{-3} to 1, ref 12
κ (/s)	Recovery of titrating species	1×10^{-3}	RNA: 10^{-5}−10^{-2}, refs 46, 47
ϕ (/s)	Degradation of regulator	1×10^{-3}	Proteins: 10^{-4}−10^{-3}, ref 12

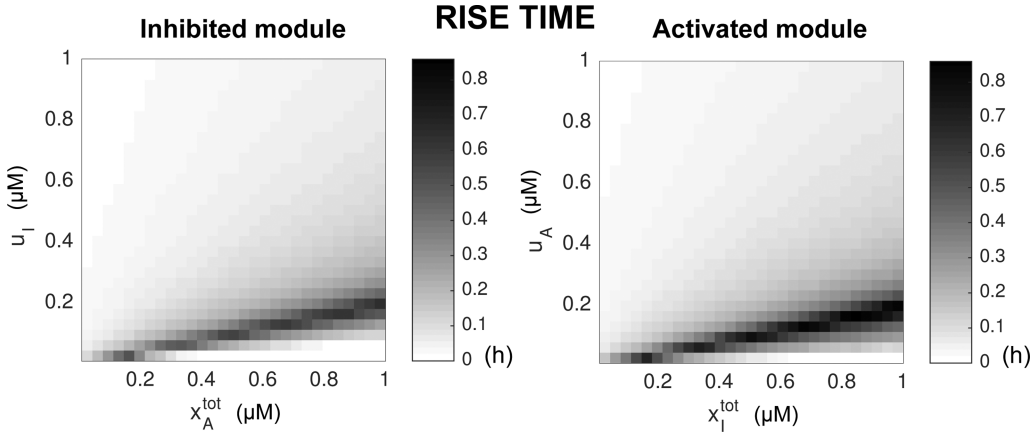

Figure 3. Rise time of the active fraction of target in the inhibited and activated module. A significant increase in rise time occurs for low values of the input source, and large concentration of constitutive activator/inhibitor. Below a certain concentration threshold of u_I and u_A, the rise time is small because the target is not affected by activation and inhibition reactions.

DOI: 10.1021/acssynbio.5b00176
ACS Synth. Biol. 2016, 5, 321−333

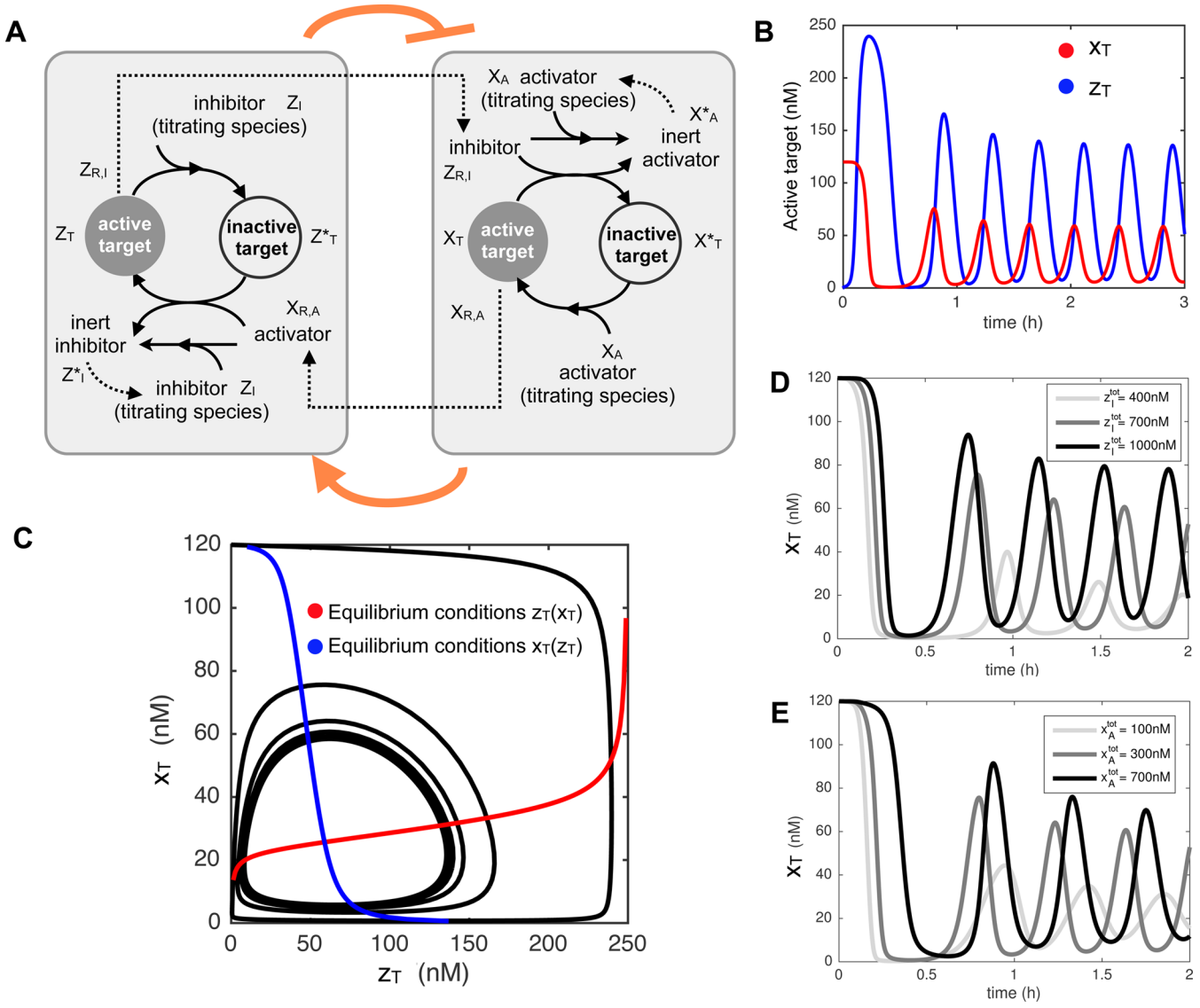

Figure 4. (A) Schematic of the oscillator system built by interconnecting an inhibited and an activated module. (B) Trajectories of the target species when eqs 7−12 are integrated using nominal parameters (Table 2). (C) Trajectories in panel B overlapped with the system equilibrium equations (Section 2.2 of the SI). (D and E) Trajectories of the target species for variable concentrations of constitutive activators and inhibitors, obtained by integrating eqs 7−12 using nominal parameters (Table 2). The concentration of titrating species affects primarily the amplitude of oscillations.

In summary, by modulating the concentration of titrating species and the titration rate, we can control the characteristics of both the dynamic and the steady state response of each module. Specifically, we can determine the threshold and steepness of the steady state nonlinearity, and we can modulate the delay of the temporal response. These features are essential to build complex dynamical systems using the titration-based modules as components.

The feedback interconnection of inhibitor and activator modules creates a negative feedback loop and is a structural oscillator. By interconnecting the inhibited and the activated module described in the previous sections, we create a negative feedback loop circuit and explore its capacity to exhibit oscillations. A scheme of the interconnection is shown in Figure 4A. The differential equations of the oscillator are

$$\dot{z}_T = \alpha_z(z_T^{tot} - z_T)x_{R,A} - \delta_z z_T z_I \quad (7)$$

$$\dot{z}_I = \kappa_z(z_I^{tot} - z_I - (z_T^{tot} - z_T)) - \delta_z z_T z_I - \nu_z x_{R,A} z_I \quad (8)$$

$$\dot{x}_{R,A} = \beta_x x_T - \alpha_z(z_T^{tot} - z_T)x_{R,A} - \nu_z x_{R,A} z_I - \phi_x x_{R,A} \quad (9)$$

$$\dot{x}_T = \alpha_x(x_T^{tot} - x_T)x_A - \delta_x x_T z_{R,I} \quad (10)$$

$$\dot{x}_A = \kappa_x(x_A^{tot} - x_A - x_T) - \alpha_x(x_T^{tot} - x_T)x_A - \nu_x x_A z_{R,I} \quad (11)$$

$$\dot{z}_{R,I} = \beta_z z_T - \delta_x x_T z_{R,I} - \nu_x x_A z_{R,I} - \phi_z z_{R,I} \quad (12)$$

The equations are ordered to highlight two groups of variables: z_T, z_I, $x_{R,A}$ and x_T, x_A, $z_{R,I}$. The first group represents the inhibited subsystem, the second group represents the activated subsystem (Figure 4A). The complete list of reactions is reported in Section 2 of the SI. First, we establish mathematically that this system has the correct structure to oscillate, and that its only admissible transition to instability is oscillatory. Second, we characterize the circuit behavior as a function of the

DOI: 10.1021/acssynbio.5b00176
ACS Synth. Biol. 2016, 5, 321−333

concentration of titrating species (constitutive activator and inhibitor), of titration reaction rate, and production rate of regulators.

Structural analysis. The oscillator is designed to have a negative feedback loop, which is generally a necessary (not sufficient) condition for oscillations. However, eqs 7−12 are nonlinear ODEs with 16 parameters, which makes the system quite complex: it is reasonable to ask what dynamic behaviors are admissible when the parameter values are varied. In addition to verifying that the system can oscillate with numerical analysis (shown in the next section), it is possible to establish analytically that−depending on the chosen parameters−this model either behaves as an oscillator, or as a system with a unique, stable equilibrium point. We can exclude multiple equilibria. We can reach this conclusion following different routes.

In the absence of titration reactions, the system is the negative feedback interconnection of two stable monotone subsystems (Section 2 of the SI). In Figure 4A, the monotone subsystems are highlighted by gray boxes; the target species x_T and z_T generate a single negative loop between the modules (orange lines). The equilibrium conditions (derived analytically for each module) intersect in a single point for arbitrary choices of the parameters. Due to the boundedness of the solution of each subsystem, the solution of ODEs (eqs 7−12) is also bounded and we can identify a "box" in the space of concentrations where the solution is trapped. These properties (together with other mild assumptions, see the SI and ref 31 for details), imply that the only type of transition to instability admitted by this system is oscillatory: in other words, by changing one or more parameters (reaction rates or total concentrations), we can push the only equilibrium admitted by the system to become unstable, and this transition is driven by a pair of complex conjugate eigenvalues which correspond to an oscillating solution. This is a behavior akin to the well-known Hopf bifurcation. We say that this is a strong candidate oscillator (Proposition 14, Section 2.1 of the SI), because the only admissible transition to instability is oscillatory.[31] This is a structural property, in the sense that it does not depend on the chosen system parameters.

When titration reactions are present the system is still a strong candidate oscillator, even though the inhibited and activated module lose their structural monotonicity properties (Section 2.2 of the SI). This can be demonstrated by computing explicitly the characteristic polynomial of the Jacobian matrix: because its coefficients are all positive (for any value of the parameters and equilibria), it cannot have nonnegative real roots (Proposition 16, Section 2.2 of the SI). Thus, unstable eigenvalues must be complex conjugate and this implies that transitions to instability can only be oscillatory. (This approach is also applied in the SI to the system in the absence of titration reactions.)

Numerical analysis. We integrate the differential eqs 7−12 numerically, and we test the capacity of the system to oscillate when certain parameters are varied. First, we randomly varied reaction rates and total concentrations of species[48,49] (Section 2.3.1 of the SI), and we used that infomation to identify a nominal set of parameters (Table 2) that yields oscillations with a period of roughly 1 h, as shown in Figure 4B. Equilibrium conditions intersect at a single equilibrium point, as expected based on our analytical derivations (Figure 4C).

Varying the concentration of titrating species affects both the amplitude and the frequency of oscillation (Figure 4D and E):

Table 2. Nominal Parameters for the Oscillator

Rate	Value	Rate	Value
α_z (/M/s)	75×10^3	α_x (/M/s)	3×10^5
δ_z (/M/s)	3×10^5	δ_x (/M/s)	3×10^5
ν_z (/M/s)	3×10^5	ν_x (/M/s)	3×10^5
β_z (/s)	5×10^{-3}	β_x (/s)	2×10^{-2}
κ_z (/s)	1×10^{-3}	κ_x (/s)	1×10^{-3}
ϕ_z (/s)	1×10^{-3}	ϕ_x (/s)	1×10^{-3}
z_T^{tot} (nM)	250	x_T^{tot} (nM)	120
z_I^{tot} (nM)	700	x_A^{tot} (nM)	300

in particular, the higher x_A^{tot} and z_I^{tot}, the larger the amplitude of oscillations. This is likely a consequence of two phenomena: the first is the temporal delay observed when the titrating species concentration increases in each module (Figure 2D, I and Figure 3A and B); the second is the steady state response threshold directly proportional to the titrating species concentration (Figure 2B, G). We explored systematically period and amplitude as a function of x_A^{tot} and z_I^{tot} in Figure 5A, for different values of the titration rate which we assumed for simplicity to be identical in both subsystems ($\nu = \nu_x = \nu_z$). All the other parameters are chosen as in Table 2. In this figure, we computed period and amplitude numerically from trajectories integrated for 20 h. These plots include also slowly damped oscillations; the region where oscillations are sustained (found as the area where the eigenvalues of the Jacobian are complex with positive real part) is inside the cyan contour. In the space x_A^{tot} and z_I^{tot}, the region where oscillations are detected becomes larger as the titration rate is increased. This is likely caused by the fact that a large titration rate sharpens the stationary and dynamic response of each module. It is worth noting that the concentration of titrating species promotes oscillations only in a certain range, which may change depending on the nominal operating point; both excess or lack of x_A^{tot} and z_I^{tot} can cause loss of oscillations.

We also varied the total concentration of targets x_T^{tot} and z_T^{tot}, and observed that the system is very sensitive to variations in the total concentration of inhibited target x_T^{tot}, which is the species responsible for creating negative feedback; in contrast, the system is robust to variations in the total concentration of activated target z_T^{tot}, as shown in Figure 5B.

The production rate of each regulator species is another particularly important parameter: the feedback interconnection of the two linearized subsystems is defined primarily by β_x and β_z, which can be thought of as parameters that control the "loop gain" of the system. This is evident from the Jacobian matrix of the system, where two blocks are interconnected precisely by β_x and β_z (SI, Sections 2.1.2 and 2.2.2). The oscillatory region in the β_x-β_z space is also increased when the titration rate is higher.

While the period is only moderately affected by the variations we considered, the amplitude changes more significantly. A complete analysis of the oscillatory regions as a function of all the system parameters is presented in the SI, Section 2.3.2. Increasing the titration rate always expands the parameter areas where oscillations are observed (Figures S3, S4, S5 and S6).

Mutually inhibiting modules create a positive feedback loop and a structural bistable system. Two inhibited modules can be mutually interconnected by designing the output of one module to be the inhibitor input of the other, as sketched in Figure 6A. The differential equations are

DOI: 10.1021/acssynbio.5b00176
ACS Synth. Biol. 2016, 5, 321−333

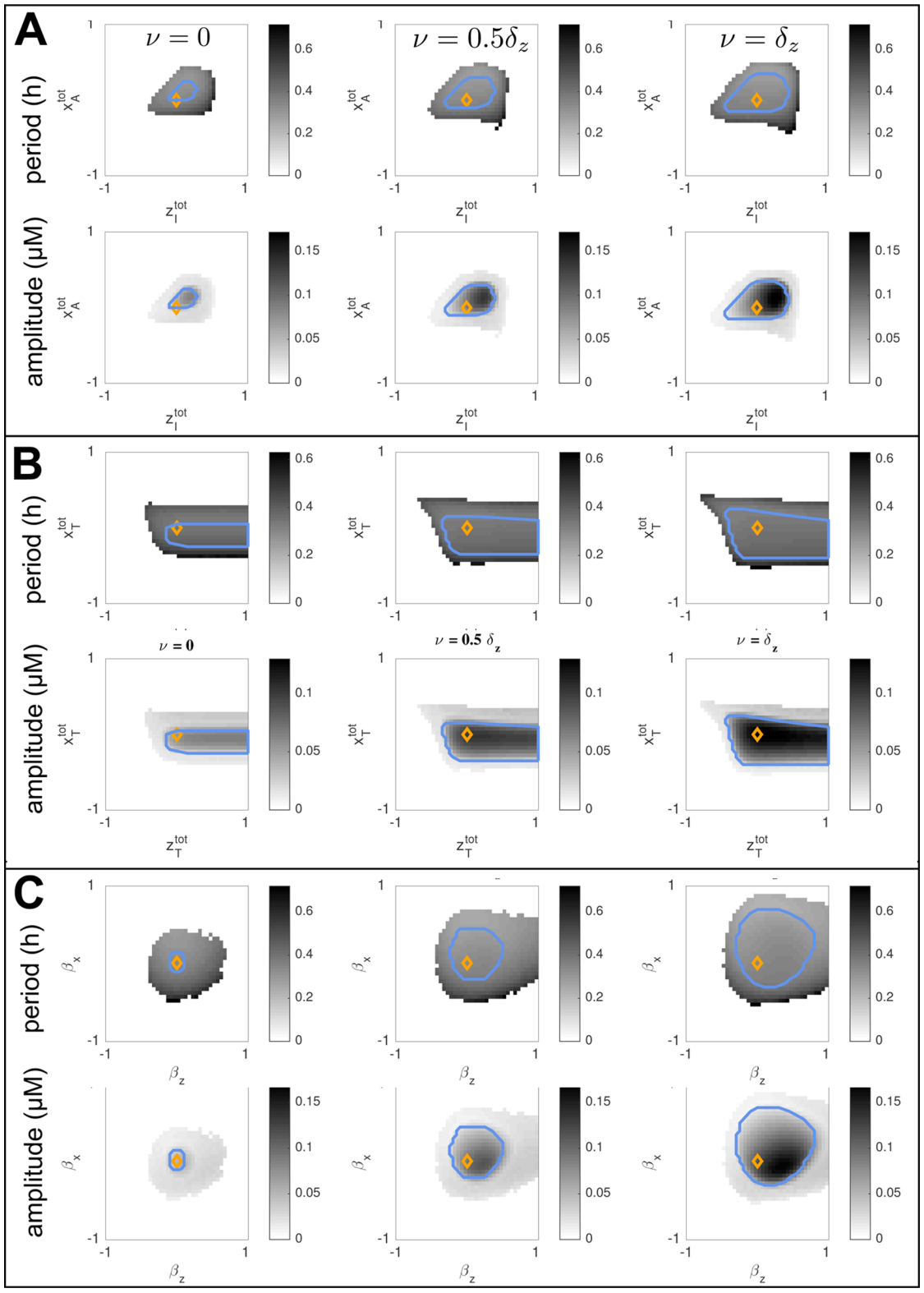

Figure 5. Period and amplitude of the oscillations when key parameters are varied near their nominal values (Table 2), for increasing value of the titration rates. Axes are in log scale; parameters are varied between one tenth and ten times their nominal values. Oscillations (sustained or damped) occur in the gray areas; the cyan contour indicates the region of sustained oscillations (the linearized system has dominant unstable complex conjugate eigenvalues); the orange diamond indicates the nominal value of the parameters. (A) Variation of the concentration of constitutive activators and inhibitors x_A^{tot} and z_I^{tot}. (B) Variations of total target concentrations x_T^{tot} and z_T^{tot}. The system is robust to variations in the target molecule of the activated subsystem. (C) Variations of the production rates of regulators, which control primarily the strength of the feedback loop. In all cases, a larger titration rate expands the oscillatory regions.

DOI: 10.1021/acssynbio.5b00176
ACS Synth. Biol. 2016, 5, 321−333

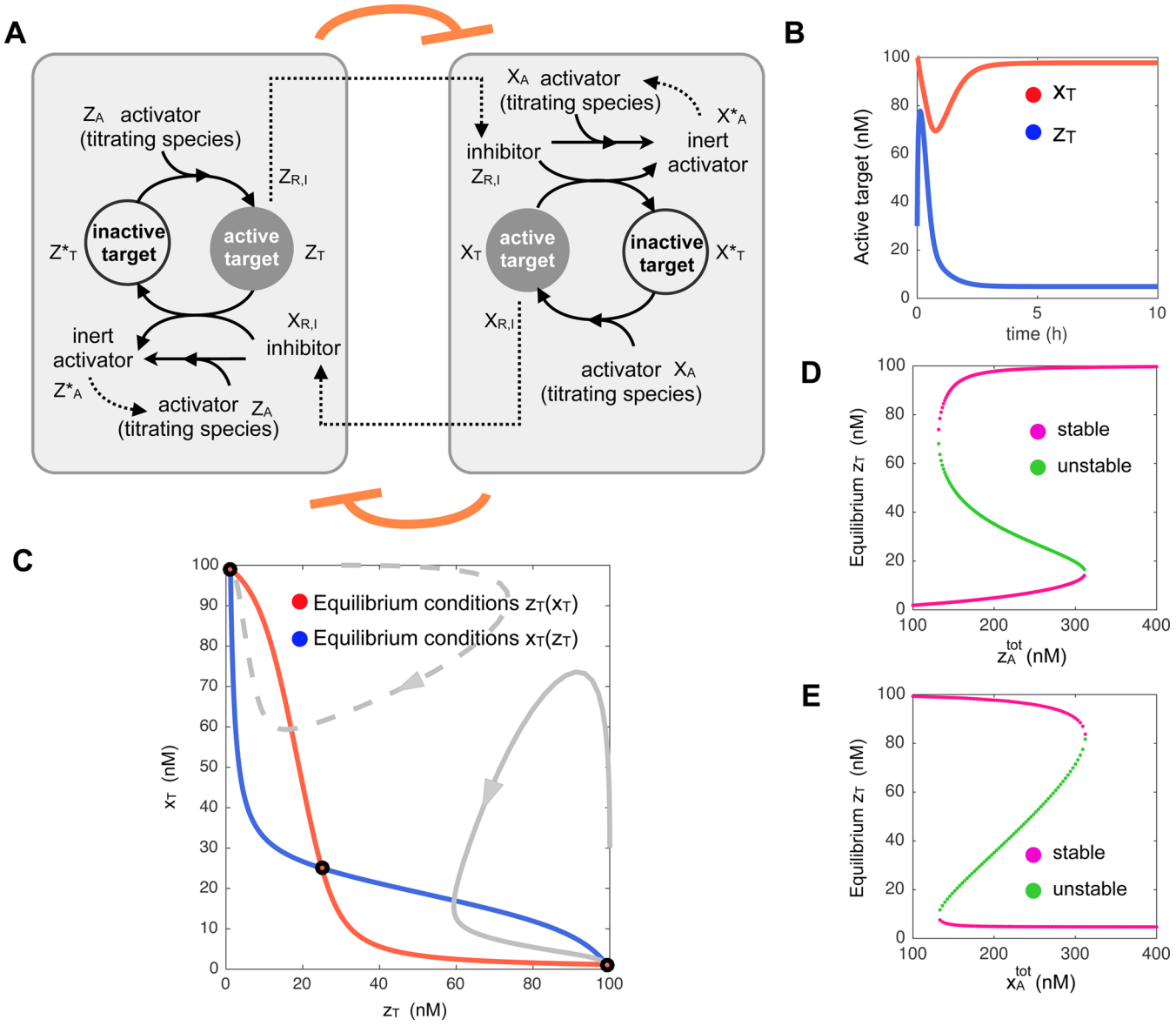

Figure 6. (A) Schematic of the bistable system built by interconnecting two inhibited modules. (B) Trajectories of the target species when eqs 13−18 are integrated using nominal parameters (Table 3). (C) Trajectories in panel B (solid gray lines) overlapped with the system equilibrium equations (Section 3.2 of the SI). (D and E) Bifurcation diagram of eqs 13−18 using nominal parameters (Table 3) for varying concentrations of the two constitutive activators.

$$\dot{z}_T = \alpha_z(z_T^{tot} - z_T)z_A - \delta_z z_T x_{R,I} \tag{13}$$

$$\dot{z}_A = \kappa_z(z_A^{tot} - z_A - z_T) - \alpha_z(z_T^{tot} - z_T)z_A - \nu_z x_{R,I} z_A \tag{14}$$

$$\dot{x}_{R,I} = \beta_x x_T - \delta_z z_T x_{R,I} - \phi_x x_{R,I} - \nu_z x_{R,I} z_A \tag{15}$$

$$\dot{x}_T = \alpha_x(x_T^{tot} - x_T)x_A - \delta_x x_T z_{R,I} \tag{16}$$

$$\dot{x}_A = \kappa_x(x_A^{tot} - x_A - x_T) - \alpha_x(x_T^{tot} - x_T)x_A - \nu_x x_A z_{R,I} \tag{17}$$

$$\dot{z}_{R,I} = \beta_z z_T - \delta_x x_T z_{R,I} - \phi_z z_{R,I} - \nu_x x_A z_{R,I} \tag{18}$$

As done for the oscillator, the variables have been grouped as z_T, z_A, $x_{R,I}$ and x_T, x_A, $z_{R,I}$ to separate the two inhibited subsystems (Figure 6A). The list of chemical reactions is reported in the SI, Section 3. In the next sections, first we establish if this system has the capacity to exhibit multistationary behaviors. Then, we explore the bistability regions as a function of various species concentrations and of the titration rate. Fast titration reaction rates always yield larger bistability regions, although this effect is less prominent than in the oscillator.

As for the oscillator circuit, the model in eqs 13−18 is quite complex: nevertheless, we can establish mathematically that for appropriate choices of parameters, the system either presents a single stable equilibrium or more than one stable equilibrium (accompanied by the emergence of unstable equilibria) where the dominant eigenvalue is real. There is no choice of the parameters that will make the system oscillate. In fact, the two inhibited modules in the absence of titration reactions are both stable, their solutions are bounded, and they are input-output monotone systems (SI, Sections 1.1 and 1.2). The two monotone modules are connected via a single positive feedback

DOI: 10.1021/acssynbio.5b00176
ACS Synth. Biol. 2016, 5, 321−333

loop; in Figure 6A, the modules are represented by components in the gray boxes; the positive feedback loop is generated by the target species and is highlighted with the orange lines. The properties satisfied by the modules imply that their interconnection (eqs 13−18) can only undergo real transitions to instability;[31] this kind of instability is related to the well-known saddle-node bifurcation. We say that this system is a strong candidate bistable system (Proposition 18 in the SI, Section 3.1.2): no matter how its reaction rates and total component concentrations are varied, the system dynamics are restricted to be either bistable or monostable.

In the presence of titration reactions, we cannot reach the same analytical conclusions without making assumptions on the region where the system equilibria fall (which depends on the specific choice of parameters). However, numerical simulations presented in the next section show that the presence of titration reactions expands the bistability region of the system significantly.

Numerical analysis. We identified a set of nominal parameters (Table 3) via a preliminary randomized exploration[48,49] of the parameter space (SI, Section 3.3.1), where for simplicity we assumed the two subsystems have the same parameters. The trajectories of x_T and z_T obtained with the nominal parameter set are shown in Figure 6B, and their behavior in phase space is shown in Figure 6C. When we vary the concentration of the titrating species near their nominal values, we obtain bifurcation diagrams that clearly show the coexistence of three equilibria, of which two are stable and one is unstable, as shown in Figure 6D and E.

Table 3. Nominal Parameters for the Bistable System

Rate	Value
$\alpha_z = \alpha_x$ (/M/s)	3×10^4
$\delta_z = \delta_x$ (/M/s)	3×10^4
$\nu_z = \nu_x = \delta_z$ (/M/s)	3×10^4
$\beta_z = \beta_x$ (/s)	0.0021
$\kappa_z = \kappa_x$ (/s)	3×10^{-4}
$\phi_z = \phi_x$ (/s)	1×10^{-3}
$z_T^{tot} = x_T^{tot}$ (nM)	100
$z_A^{tot} = x_A^{tot}$ (nM)	200

We then explored bistability trends in the region near the nominal parameters (Table 3). Bistability regions were computed by numerically finding the intersections of the equilibrium conditions, and then checking the magnitude of the eigenvalues of the Jacobian matrix computed at the equilibrium (see SI, Section 3.3.2 for further details). In Figure 7 we vary the concentration of titrating species, of targets, and the regulator production rates (all other parameters are kept constant as in Table 3). First of all, we note that in the absence of titration reactions ($\nu_x = \nu_z = 0$), the system becomes very sensitive to variations in the concentration of titrating species, and the region of bistability is very narrow; this limitation can be relaxed by increasing the titration rate (Figure 7A). In contrast, the concentration of target species can significantly vary without affecting bistability, and again a fast titration rate expands the bistable region. Similarly, changes in the regulator production rates (which determine the strength of the feedback loop) are tolerated in a reasonably large range, as long as the rates remain large. As in the oscillator, increasing the titration rate always broadens the bistable regime; this is verified numerically for all other parameters in the sysem (SI, Section 3.3.2, Figures S7, S8, S9 and S10).

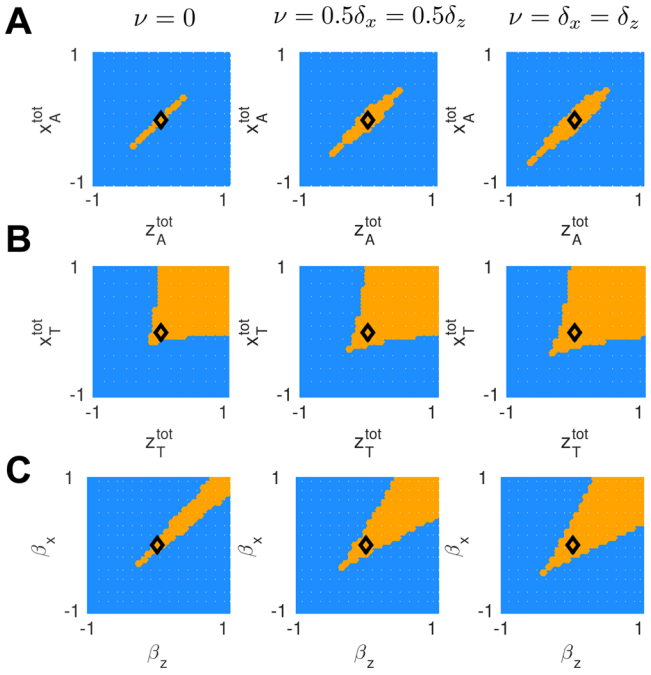

Figure 7. Regions of bistability near the nominal parameters (Table 3) for increasing value of the titration rates; we assume the two inhibited subsystems have identical parameters for simplicity. Axes are in log scale; parameters are varied between one tenth and ten times their nominal values. (A) Variations in the concentration of constitutive activators; the bistability region is very narrow, but can be expanded by increasing the titration rate. (B) Bistability region as a function of the total target concentration. (C) Bistability region as a function of the regulator production rates β_x and β_z which control the strength of the feedback loop (Section 3 of the SI).

DISCUSSION AND CONCLUSIONS

We have demonstrated that biomolecular modules regulated by monomeric inputs can be successfully interconnected to build two essential circuit components: an oscillator and a bistable switch. We considered deterministic ODE models of these modules, which are composed of a target molecule and of its constitutive regulators (activators or inhibitors); input regulators compete with the constitutive regulators, which act as titrating species for the input, to determine the active or inactive state of the target. The steady state and transient response of the target molecule concentration can be finely tuned by appropriate design of the titration rate and the concentration of the titrating species. Specifically, these parameters determine the "dead-zone" and steepness of the on/off transitions in the steady state dose response, and the speed and delay of the dynamic response, which promote the emergence of oscillations and bistability when modules are interconnected in feedback loops. One important finding is that, although direct titration reactions significantly increase the probability of the circuits to oscillate or have multiple steady states, they are not strictly necessary to provide the systems with the capacity for these complex behaviors.

Our numerical simulations are accompanied by rigorous mathematical analysis: we show that the modules and their interconnections have many important properties that do not depend on the model parameters (reaction rates and total

DOI: 10.1021/acssynbio.5b00176
ACS Synth. Biol. 2016, 5, 321−333

concentrations of components). We say that our analysis is structural precisely because it allows us to establish the properties of the systems that hold for arbitrary parameter values; this approach can yield useful insights in nonlinear systems with many parameters. In particular, we show that in the absence of direct titration the modules are bounded and stable input−output monotone systems[27,30] under very mild assumptions (the concentration of constitutive regulators should be larger than the concentration of their target molecule). These properties guarantee that when a positive or negative feedback loop is generated by their interconnection, the admissible bifurcations in the system are either exclusively multistationary (positive feedback) or exclusively oscillatory (negative feedback). These results build on previous theoretical work[31] where a complete classification of oscillatory and multistationary systems is proposed based on Jacobian cycles. The presence of titration reactions weakens these structural properties, making them dependent on the location of the equilibria and on the strength of the titration rate. However, numerical simulations show that titration increases the probability of bistability and oscillations, because it sharpens the stationary and temporal response of the modules, and increases the delay in the system.

In addition to the concentration of titrating species and the titration rates, the key parameters in the modules are the production rates of the regulators β_x and β_z. These rates primarily influence the strength of the feedback loops, both in the oscillator and in the bistable system, as can be seen from the linearization of the modules' ODEs shown in the SI, Sections 2 and 3. High gain in a feedback loop can generally destabilize a dynamical system; however, β_x and β_z influence other parts of the linearized dynamics as well. Thus their increase does not guarantee that the desired bifurcation will occur.

While it is well known (experimentally and theoretically) that molecular titration can be tuned to generate nonlinear ultrasensitive responses and delays,[12,13,50] to our knowledge not many attempts have been made to build complex dynamic networks using this mechanism. Experimentally, molecular titration obtained via RNA polymerase sigma factors was used *in vivo* to build a bistable switch with tunable domain boundaries and the capacity for state toggling.[51] *In vitro*, titration pathways very similar to those we describe here were used to build a bistable switch[28] and an oscillator.[23,24] In these systems, the target molecules are DNA templates that produce RNA outputs acting as mutual template regulators; template activity is switched on and off via a partial promoter displacement reaction, whose speed is determined by sequence and length of toehold domains on the nicked promoter (Figure 1B). In these systems, templates are constitutively activated or repressed depending on the presence of DNA activators (which complete the promoter) and DNA inhibitors (which displace the activators). RNA regulators either inhibit (by displacing DNA activators) or activate (by displacing DNA inhibitors) the templates, generating inert activator or inhibitor complexes which can be recovered by RNase H-mediated degradation of RNA bound to DNA. By increasing the concentration of titrating species (DNA activators/inhibitors) within certain bounds, the oscillatory or bistable behavior of the systems is significantly enhanced.[24] The molecular oscillator is also highly sensitive to the concentration of RNA polymerase, which in the system determines the production rates. These experimental findings are consistent with the results of our analysis.

A common feature of existing dynamic systems built using molecular titration[23,24,28,51] is that the domains in parameter space where oscillations or bistability are achieved are generally narrow. Recently, this was clearly highlighted in a series of experiments where the *in vitro* oscillator by Kim and Winfree was encapsulated in microdroplets;[52] the droplet production process causes a perturbation of the nominal operating point of the system (in particular, there is a loss of enzymes' activity) and results in a striking dynamical diversity and often a loss of oscillations in droplets. This is consistent with our numerical analysis, and we speculate that this might be a consequence of the monomeric nature of the regulators in the system. In a regime where stochastic effects are predominant, however, the lack of cooperativity may not be a significant limitation to achieve complex behaviors, depending on the system architecture.[53,54]

We expect that our analysis of molecular titration in the context of feedback systems will be useful to build circuits with new classes of monomeric regulators such as the CRISPR-Cas system (Figure 1D). Logic circuits based on CRISPR-Cas have been recently characterized;[10,55] however, feedback loops with bistable or oscillatory responses have not yet been obtained, presumably due to the difficulty in obtaining sharp nonlinear responses required for these behaviors. While building circuits with multiple, interconnected feedback loops may prove helpful,[56] we speculate that titration of the guide RNA with overexpressed titrating RNA species might be an effective strategy.

■ ASSOCIATED CONTENT

Supporting Information

The Supporting Information is available free of charge on the ACS Publications website at DOI: 10.1021/acssynbio.5b00176.

Detailed information on our mathematical analysis, numerical simulations and additional references are included in the Supporting Information file. (PDF)

■ AUTHOR INFORMATION

Corresponding Author

*E-mail: efranco@engr.ucr.edu.

Notes

The authors declare no competing financial interest.

■ ACKNOWLEDGMENTS

This work has been supported by the National Science Foundation through grant CMMI-1266402.

■ REFERENCES

(1) Elowitz, M. B., and Leibler, S. (2000) A synthetic oscillatory network of transcriptional regulators. *Nature 403*, 335−338.

(2) Gardner, T. S., Cantor, C. R., and Collins, J. J. (2000) Construction of a genetic toggle switch in *Escherichia coli*. *Nature 403*, 339−342.

(3) Way, J. C., Collins, J. J., Keasling, J. D., and Silver, P. A. (2014) Integrating biological redesign: where synthetic biology came from and where it needs to go. *Cell 157*, 151−161.

(4) Lucks, J. B., Qi, L., Mutalik, V. K., Wang, D., and Arkin, A. P. (2011) Versatile RNA-sensing transcriptional regulators for engineering genetic networks. *Proc. Natl. Acad. Sci. U. S. A. 108*, 8617−8622.

(5) Galloway, K. E., Franco, E., and Smolke, C. D. (2013) Dynamically reshaping signaling networks to program cell fate via genetic controllers. *Science 341*, 6152.

DOI: 10.1021/acssynbio.5b00176
ACS Synth. Biol. 2016, 5, 321−333

(6) Rodrigo, G., Landrain, T. E., and Jaramillo, A. (2012) De novo automated design of small RNA circuits for engineering synthetic riboregulation in living cells. *Proc. Natl. Acad. Sci. U. S. A. 109*, 15271−15276.
(7) Qi, L. S., and Arkin, A. P. (2014) A versatile framework for microbial engineering using synthetic non-coding RNAs. *Nat. Rev. Microbiol. 12*, 341−354.
(8) Green, A. A., Silver, P. A., Collins, J. J., and Yin, P. (2014) Toehold switches: de-novo-designed regulators of gene expression. *Cell 159*, 925−939.
(9) Qi, L. S., Larson, M. H., Gilbert, L. A., Doudna, J. A., Weissman, J. S., Arkin, A. P., and Lim, W. A. (2013) Repurposing CRISPR as an RNA-guided platform for sequence-specific control of gene expression. *Cell 152*, 1173−1183.
(10) Nielsen, A. A., and Voigt, C. A. (2014) Multi-input CRISPR/Cas genetic circuits that interface host regulatory networks. *Mol. Syst. Biol. 10*, 11.
(11) Prinz, H. (2010) Hill coefficients, dose-response curves and allosteric mechanisms. *Journal of Chemical Biology 3*, 37−44.
(12) Buchler, N. E., and Louis, M. (2008) Molecular Titration and Ultrasensitivity in Regulatory Networks. *J. Mol. Biol. 384*, 1106−1119.
(13) Buchler, N. E., and Cross, F. R. (2009) Protein sequestration generates a flexible ultrasensitive response in a genetic network. *Mol. Syst. Biol. 5*, 272.
(14) Hughes, K. T., and Mathee, K. (1998) The anti-sigma factors. *Annu. Rev. Microbiol. 52*, 231−286.
(15) Yanagita, M. (2005) BMP antagonists: their roles in development and involvement in pathophysiology. *Cytokine Growth Factor Rev. 16*, 309−317.
(16) Stricker, J., Cookson, S., Bennett, M. R., Mather, W. H., Tsimring, L. S., and Hasty, J. (2008) A fast, robust and tunable synthetic gene oscillator. *Nature 456*, 516−519.
(17) Yang, Q., and Ferrell, J. E., Jr (2013) The Cdk1-APC/C cell cycle oscillator circuit functions as a time-delayed, ultrasensitive switch. *Nat. Cell Biol. 15*, 519−525.
(18) Goldbeter, A. *Biochemical Oscillations and Cellular Rhythms: The Molecular Bases of Periodic and Chaotic Behaviour*; Cambridge University Press: 1997.
(19) Atkinson, M. R., Savageau, M., Myers, J., and Ninfa, A. (2003) Development of genetic circuitry exhibiting toggle switch or oscillatory behavior in *Escherichia coli*. *Cell 113*, 597−607.
(20) Fung, E., Wong, W. W., Suen, J. K., Bulter, T., Lee, S.-G., and Liao, J. C. (2005) A synthetic gene-metabolic oscillator. *Nature 435*, 118−122.
(21) Tigges, M., Marquez-Lago, T. T., Stelling, J., and Fussenegger, M. (2009) A tunable synthetic mammalian oscillator. *Nature 457*, 309−312.
(22) Danino, T., Mondragon-Palomino, O., Tsimring, L., and Hasty, J. (2010) A synchronized quorum of genetic clocks. *Nature 463*, 326−330.
(23) Kim, J., and Winfree, E. (2011) Synthetic *in vitro* transcriptional oscillators. *Mol. Syst. Biol. 7*, 465.
(24) Franco, E., Friedrichs, E., Kim, J., Jungmann, R., Murray, R., Winfree, E., and Simmel, F. C. (2011) Timing molecular motion and production with a synthetic transcriptional clock. *Proc. Natl. Acad. Sci. U. S. A. 108*, E784−E793.
(25) Montagne, K., Plasson, R., Sakai, Y., Fujii, T., and Rondelez, Y. (2011) Programming an *in vitro* DNA oscillator using a molecular networking strategy. *Mol. Syst. Biol. 7*, 466.
(26) Ferrell, J. E. (2002) Self-perpetuating states in signal transduction: positive feedback, double-negative feedback and bistability. *Curr. Opin. Cell Biol. 14*, 140−148.
(27) Angeli, D., and Sontag, E. (2003) Monotone control systems. *IEEE Trans. Autom. Control 48*, 1684−1698.
(28) Kim, J., White, K. S., and Winfree, E. (2006) Construction of an *in vitro* bistable circuit from synthetic transcriptional switches. *Mol. Syst. Biol. 2*, 68.
(29) Padirac, A., Fujii, T., and Rondelez, Y. (2012) Bottom-up construction of *in vitro* switchable memories. *Proc. Natl. Acad. Sci. U. S. A. 109*, E3212−E3220.
(30) Angeli, D., Ferrell, J. E., and Sontag, E. D. (2004) Detection of multistability, bifurcations, and hysteresis in a large class of biological positive-feedback systems. *Proc. Natl. Acad. Sci. U. S. A. 101*, 1822−1827.
(31) Blanchini, F., Franco, E., and Giordano, G. (2014) A structural classification of candidate oscillatory and multistationary biochemical systems. *Bull. Math. Biol. 76*, 2542−2569.
(32) Thomas, R. In *Springer Series in Synergetics*; Della-Dora, J., Demongeot, J., Lacolle, B., Eds.; Springer-Verlag: 1981; Vol. *9*, pp 180−193.
(33) Gouze, J.-L. (1998) Positive and negative circuits in dynamical systems. *J. Biol. Syst. 6*, 11−15.
(34) Snoussi, E. (1998) Necessary conditions for multistationarity and stable periodicity. *J. Biol. Syst. 6*, 3−9.
(35) Waters, L. S., and Storz, G. (2009) Regulatory RNAs in bacteria. *Cell 136*, 615−628.
(36) Hsu, P. D., Lander, E. S., and Zhang, F. (2014) Development and applications of CRISPR-Cas9 for genome engineering. *Cell 157*, 1262−1278.
(37) Schmiedel, J. M., Axmann, I. M., and Legewie, S. (2012) Multi-target regulation by small RNAs synchronizes gene expression thresholds and may enhance ultrasensitive behavior. *PLoS One 7*, e42296.
(38) Yurke, B., and Mills, A. P. (2003) Using DNA to power nanostructures. *Genetic Programming and Evolvable Machines 4*, 111−122.
(39) Hsiao, V., de los Santos, E. L., Whitaker, W. R., Dueber, J. E., and Murray, R. M. (2014) Design and implementation of a biomolecular concentration tracker. *ACS Synth. Biol. 4*, 150−161.
(40) Franco, E., Giordano, G., Forsberg, P.-O., and Murray, R. M. (2014) Negative autoregulation matches production and demand in synthetic transcriptional networks. *ACS Synth. Biol. 3*, 589−599.
(41) Angeli, D., and Sontag, E. (2008) Oscillations in I/O monotone systems. *IEEE Trans. Autom. Control 55*, 166−176.
(42) Zhang, D. Y., Turberfield, A. J., Yurke, B., and Winfree, E. (2007) Engineering entropy-driven reactions and networks catalyzed by DNA. *Science 318*, 1121−1125.
(43) Schlosshauer, M., and Baker, D. (2004) Realistic protein-protein association rates from a simple diffusional model neglecting long-range interactions, free energy barriers, and landscape ruggedness. *Protein Sci. 13*, 1660−1669.
(44) Schreiber, G., Haran, G., and Zhou, H.-X. (2009) Fundamental aspects of protein-protein association kinetics. *Chem. Rev. 109*, 839−860.
(45) Vogel, U., and Jensen, K. F. (1994) The RNA chain elongation rate in *Escherichia coli* depends on the growth rate. *J. Bacteriol. 176*, 2807−2813.
(46) Chen, H., Shiroguchi, K., Ge, H., and Xie, X. S. (2015) Genome-wide study of mRNA degradation and transcript elongation in *Escherichia coli*. *Mol. Syst. Biol. 11*, 781.
(47) Beelman, C. A., and Parker, R. (1995) Degradation of mRNA in eukaryotes. *Cell 81*, 179−183.
(48) Cuba, C. E., Valle, A. R., Ayala-Charca, G., Villota, E. R., and Coronado, A. M. (2015) Influence of parameter values on the oscillation sensitivities of two p53-Mdm2 models. *Systems and Synthetic Biology 9*, 77−84.
(49) Blanchini, F., Samaniego, C. C., Franco, E., Giordano, G. Design of a molecular clock with RNA-mediated regulation. *Proceedings of the IEEE Conference on Decision and Control*. 2014; pp 4611−4616.
(50) Ricci, F., Vallée-Bélisle, A., and Plaxco, K. W. (2011) High-precision, *in vitro* validation of the sequestration mechanism for generating ultrasensitive dose-response curves in regulatory networks. *PLoS Comput. Biol. 7*, e1002171.
(51) Chen, D., and Arkin, A. P. (2012) Sequestration-based bistability enables tuning of the switching boundaries and design of a latch. *Mol. Syst. Biol. 8*, 1.

DOI: 10.1021/acssynbio.5b00176
ACS Synth. Biol. 2016, 5, 321−333

(52) Weitz, M., Kim, J., Kapsner, K., Winfree, E., Franco, E., and Simmel, F. C. (2014) Diversity in the dynamical behaviour of a compartmentalized programmable biochemical oscillator. *Nat. Chem. 6*, 295−302.
(53) To, T. L., and Maheshri, N. (2010) Noise can induce bimodality in positive transcriptional feedback loops without bistability. *Science 327*, 1142−1145.
(54) Lipshtat, A., Loinger, A., Balaban, N. Q., and Biham, O. (2006) Genetic toggle switch without cooperative binding. *Phys. Rev. Lett. 96*, 188101.
(55) Bikard, D., Jiang, W., Samai, P., Hochschild, A., Zhang, F., and Marraffini, L. A. (2013) Programmable repression and activation of bacterial gene expression using an engineered CRISPR-Cas system. *Nucleic Acids Res. 41*, 7429−7437.
(56) Lebar, T., et al. (2014) A bistable genetic switch based on designable DNA-binding domains. *Nat. Commun. 5*, 5007.

DOI: 10.1021/acssynbio.5b00176
ACS Synth. Biol. 2016, 5, 321−333

Molecular titration promotes oscillations and bistability in minimal network models with monomeric regulators

—

Supplementary Information

Christian Cuba Samaniego[1], Giulia Giordano[2], Jongmin Kim[3], Franco Blanchini[2], and Elisa Franco[1,*]

[1] *Department of Mechanical Engineering, University of California at Riverside, 900 University Avenue, Riverside, CA 92521, USA*

[2] *Department of Mathematics and Computer Science, University of Udine, via delle Scienze 206, 33100 Udine, Italy*

[3] *Wyss Institute for Biologically Inspired Engineering, Harvard University, 3 Blackfan Circle, Boston, MA 02115, USA*

[*] *Corresponding author*

Contents

1 Analysis of the inhibited and activated modules

The oscillator and the bistable systems considered in the main paper can be analyzed following the theory proposed in [1, 2], which allows us to show that they structurally have (by design) the capacity to respectively exhibit oscillations and bistability.

On the one hand, it can be shown that a system given by the feedback interconnection of an inhibitor module and an activator module is the negative feedback interconnection of two monotone systems, and is therefore a strong candidate oscillator according to [2] (if driven to instability, the system necessarily exhibits sustained oscillations). On the other hand, a system given by the feedback interconnection of mutually inhibiting modules is the positive feedback interconnection of two monotone systems, and is therefore a strong candidate bistable system according to [2] (if the system is driven to instability, bistable phenomena necessarily arise).

Here we demonstrate the same properties following an alternative, simplified route. We begin by analyzing the properties of the inhibited and the activated modules individually.

1.1 Analysis of the inhibited module

1.1.1 Analysis in the absence of direct titration reaction

We recall the model for the inhibited module:

$$\dot{x}_T = \alpha(x_T^{tot} - x_T)x_A - \delta x_T r_I \tag{1}$$
$$\dot{x}_A = \kappa(x_A^{tot} - x_A - x_T) - \alpha(x_T^{tot} - x_T)x_A \tag{2}$$
$$\dot{r}_I = \beta u_I - \delta x_T r_I - \phi r_I. \tag{3}$$

Assumption 1. *We assume that* $x_A^{tot} \geq x_T^{tot}$.

Additionally, we make an assumption that relates parameters κ, α, and the total concentrations of target and constitutive activator.

Assumption 2. *We assume that* $x_A^{tot} - x_T^{tot} - \frac{\kappa}{\alpha} \geq 0$.

Proposition 1. *For a given concentration of inhibitor source* $\bar{u}_I$*, system* (1)–(3) *has unique equilibrium values* $\bar{x}_T$*,* $\bar{x}_A$ *and* $\bar{r}_I$*. The equilibrium* $\bar{x}_T$ *is a monotonic, strictly decreasing function of* $\bar{u}_I$*.*

Proof. We first find an expression of $\bar{x}_A$ as a function of $\bar{x}_T$. From $\dot{x}_A = 0$, we obtain:

$$\bar{x}_A(\bar{x}_T) = \frac{\kappa(x_A^{tot} - \bar{x}_T)}{\alpha(x_T^{tot} - \bar{x}_T) + \kappa} \doteq g_A(\bar{x}_T).$$

It can be verified that under Assumptions 1 and 2, $\partial g_A(\bar{x}_T)/\partial \bar{x}_T \geq 0$. Thus $g_A(\bar{x}_T)$ is a continuous, monotonically increasing function of $\bar{x}_T$, and, for a given value of u_I, $\bar{x}_T$, there is a unique equilibrium $\bar{x}_A$.

Now we find $\bar{r}_I$ as a function of $\bar{x}_T$. From $\dot{x}_T = 0$, We obtain:

$$\bar{r}_I(\bar{x}_T) = \frac{\alpha(x_T^{tot} - \bar{x}_T)\bar{x}_A(\bar{x}_T)}{\delta \bar{x}_T} = \frac{\alpha(x_T^{tot} - \bar{x}_T)}{\delta \bar{x}_T} \frac{\kappa(x_A^{tot} - \bar{x}_T)}{\alpha(x_T^{tot} - \bar{x}_T) + \kappa}$$
$$= \frac{\kappa}{\delta} \frac{(x_A^{tot} - \bar{x}_T)}{\bar{x}_T} \frac{(x_T^{tot} - \bar{x}_T)}{(x_T^{tot} - \bar{x}_T) + \frac{\kappa}{\alpha}} \doteq \frac{\kappa}{\delta} A(\bar{x}_T)\, B(\bar{x}_T),$$

where $A(\bar{x}_T) \doteq \frac{(x_A^{tot} - \bar{x}_T)}{\bar{x}_T}$ and $B(\bar{x}_T) \doteq \frac{(x_T^{tot} - \bar{x}_T)}{(x_T^{tot} - \bar{x}_T) + \frac{\kappa}{\alpha}}$. Since $\partial A/\partial \bar{x}_T = -\frac{x_A^{tot}}{\bar{x}_T^2} < 0$, $\partial B/\partial \bar{x}_T = -\frac{\frac{\kappa}{\alpha}}{(x_T^{tot} - \bar{x}_T + \frac{\kappa}{\alpha})^2} < 0$, and both $A(\bar{x}_T)$ and $B(\bar{x}_T)$ are positive for arbitrary parameter values (except at $\bar{x}_T = x_T^{tot}$, where $B(\bar{x}_T) = 0$),

we can conclude that the partial derivative $\partial \bar{r}_I(\bar{x}_T)/\partial \bar{x}_T = \frac{\kappa}{\delta}\left[(\partial A/\partial \bar{x}_T)\, B(\bar{x}_T) + A(\bar{x}_T)(\partial B/\partial \bar{x}_T)\right] < 0$, thus $\bar{r}_I$ is a monotonic, strictly decreasing function of $\bar{x}_T$.

Finally, from $\dot{r}_I = 0$ we find

$$\bar{u}_I = \frac{1}{\beta}(\delta \bar{x}_T + \phi)\bar{r}_I(\bar{x}_T) \doteq h(\bar{x}_T).$$

To verify that the introduced function $h(\bar{x}_T)$ is a strictly decreasing monotonic function of $\bar{x}_T$, we rewrite it as $h(\bar{x}_T) = \frac{1}{\beta}\left[\delta \bar{x}_T \bar{r}_I(\bar{x}_T) + \phi \bar{r}_I(\bar{x}_T)\right] = \frac{1}{\beta}\left[C(\bar{x}_T) + \phi r_I(\bar{x}_T)\right]$. Because β and ϕ are positive constants, and we already verified that $\partial \bar{r}_I(\bar{x}_T)/\partial \bar{x}_T < 0$, we only need to check that $\partial C(\bar{x}_T)/\partial \bar{x}_T < 0$. It is sufficient to note that $C(\bar{x}_T) = \kappa(x_A^{tot} - \bar{x}_T)B(\bar{x}_T)$ (see definition of $B(\bar{x}_T)$ above). Since $(\partial B/\partial \bar{x}_T) < 0$, $\partial(x_A^{tot} - \bar{x}_T)/\partial \bar{x}_T < 0$, and both $B(\bar{x}_T) > 0$ and $(x_A^{tot} - \bar{x}_T) > 0$, we have that $\partial C(\bar{x}_T)/\partial \bar{x}_T < 0$.

Being $h(\bar{x}_T)$ a continuous, monotonic, strictly deceasing function of $\bar{x}_T$, its inverse is also a continuous, monotonic, decreasing function: $\bar{x}_T = g(\bar{u}_I) = h^{-1}(\bar{u}_I)$. We conclude that the equilibrium $\bar{x}_T$ for a given $\bar{u}_I$ is unique, and so are the other equilibria $\bar{x}_A$ and $\bar{r}_I$. In particular, the higher the concentration of input U_I, the smaller the equilibrium concentration of X_T. □

We can show that a suitable set is positively invariant for the system: namely, any trajectory starting in this set is confined in the set for all time instants.

Proposition 2. *The set*

$$0 \le x_T \le x_T^{tot}, \qquad \frac{\kappa}{\alpha} \le x_A \le x_A^{tot}, \qquad r_I \ge 0 \tag{4}$$

is positively invariant [3] for the system (1)–(3) *for any* u_I.

Proof. Since all the variables are non–negative and the variables x_T and x_A cannot exceed their total values, all the constraints are obvious with the exception of $x_A \ge \kappa/\alpha$. We show that this constraint cannot be violated: if we start with $x_A(0) \ge \kappa/\alpha$, then the constraint is satisfied for all $t > 0$. In fact, for $x_A = \kappa/\alpha$ we have

$$\dot{x}_A = \kappa(x_A^{tot} - \kappa/\alpha - x_T) - \alpha(x_T^{tot} - x_T)(\kappa/\alpha) = \kappa(x_A^{tot} - x_T^{tot} - \kappa/\alpha) \ge 0$$

due to Assumption 2. □

Proposition 3. *The solutions of system* (1)–(3) *are bounded.*

Proof. Species x_T and x_A are bounded by assumption. The dynamics of the regulator satisfies the inequality $\dot{r}_I(t) \le \beta u_I^{max} - \phi r_I$. By applying the comparison principle [6], we conclude that

$$r_I(t) \le r_I(0)e^{-\phi t} + \beta u_I^{max}(1 - e^{-\phi t})/\phi,$$

which ensures $r_I(t) \le \max\{r_I(0), \beta u_I^{max}/\phi\}$ at any point in time. □

Proposition 4. *The unique equilibrium of system* (1)–(3) *is locally stable.*

Proof. For a given input u_I, the system admits a unique equilibrium (see Proposition 1). The Jacobian matrix

$$J_I = \begin{bmatrix} -(\alpha \bar{x}_A + \delta \bar{r}_I) & \alpha(x_T^{tot} - \bar{x}_T) & -\delta \bar{x}_T \\ -\kappa + \alpha \bar{x}_A & -[\kappa + \alpha(x_T^{tot} - \bar{x}_T)] & 0 \\ -\delta \bar{r}_I & 0 & -(\delta \bar{x}_T + \phi) \end{bmatrix}$$

can be recast as a Metzler matrix (namely, a matrix whose non–diagonal entries are nonnegative) by changing the sign to the last row and column; in fact term $\alpha \bar{x}_A - \kappa > 0$ in view of Proposition 2. A Metzler matrix has exclusively eigenvalues with negative real part (hence, is stable) if and only if all the coefficients of its characteristic polynomial $\det(\lambda I - J_I)$ are positive. A computation of the characteristic polynomial of J_I shows that all its coefficients are positive. □

Remark 1. *Systems whose Jacobian is (or is similar, up to a change of sign, to) a Metzler matrix are called monotone. As we will show later, in the absence of titration both the oscillator and the bistable system can be seen as the interconnection of two monotone components (corresponding to the modules).*

1.1.2 Analysis in the presence of direct titration reactions

When titration reactions are present, the equations describing the system become:

$$\dot{x}_T = \alpha(x_T^{tot} - x_T)x_A - \delta x_T r_I \tag{5}$$
$$\dot{x}_A = \kappa(x_A^{tot} - x_A - x_T) - \alpha(x_T^{tot} - x_T)x_A - \nu x_A r_I \tag{6}$$
$$\dot{r}_I = \beta u_I - \delta x_T r_I - \phi r_I - \nu x_A r_I. \tag{7}$$

Proposition 5. *The solutions of system* (5)–(7) *are globally bounded.*

Proof. All of the variables are non–negative and the variables x_T and x_A are upper–bounded by their total values x_T^{tot} and x_A^{tot}. The boundedness of r_I can be proved resorting to the comparison principle, as previously done for the system in the absence of titration. □

Equilibria: First we find an expression for $\bar{x}_A$ as a function of $\bar{x}_T$. From $\dot{x}_T + \dot{x}_A = 0$, we obtain:

$$\kappa(x_A^{tot} - \bar{x}_A - \bar{x}_T) = (\delta\bar{x}_T + \nu\bar{x}_A)\bar{r}_I,$$

and from $\dot{x}_T = 0$,

$$\alpha(x_T^{tot} - \bar{x}_T)\bar{x}_A = \delta\bar{x}_T\bar{r}_I.$$

Then

$$\bar{r}_I = \frac{\alpha(x_T^{tot} - \bar{x}_T)\bar{x}_A}{\delta\bar{x}_T} = \frac{\kappa(x_A^{tot} - \bar{x}_A - \bar{x}_T)}{\delta\bar{x}_T + \nu\bar{x}_A}.$$

We obtain a second order polynomial of the following form: $a_x\bar{x}_A^2 + b_x\bar{x}_A + c_x = 0$, where

$$a_x = \frac{\alpha\nu(x_T^{tot} - \bar{x}_T)}{\delta\bar{x}_T}, \quad b_x = \alpha(x_T^{tot} - \bar{x}_T) + \kappa, \quad c_x = -\kappa(x_A^{tot} - \bar{x}_T).$$

Since c_x is always negative, there is a unique positive and acceptable solution:

$$\bar{x}_A(\bar{x}_T) = \frac{-b_x + \sqrt{b_x^2 - 4a_xc_x}}{2a_x}.$$

With this expression we can find $\bar{r}_I$ as a function of $\bar{x}_T$. From $\dot{x}_T = 0$, we obtain:

$$\bar{r}_I(\bar{x}_T) = \frac{\alpha(x_T^{tot} - \bar{x}_T)\bar{x}_A(\bar{x}_T)}{\delta\bar{x}_T}.$$

From $\dot{r}_I = 0$,

$$\bar{u}_I = \frac{1}{\beta}(\delta\bar{x}_T + \phi + \nu\bar{x}_A(\bar{x}_T))\bar{r}_I(\bar{x}_T).$$

Jacobian analysis: The Jacobian matrix becomes:

$$J_I = \begin{bmatrix} -(\alpha\bar{x}_A + \delta\bar{r}_I) & \alpha(x_T^{tot} - \bar{x}_T) & -\delta\bar{x}_T \\ -\kappa + \alpha\bar{x}_A & -[\kappa + \alpha(x_T^{tot} - \bar{x}_T) + \nu\bar{r}_I] & -\nu\bar{x}_A \\ -\delta\bar{r}_I & -\nu\bar{r}_I & -(\delta\bar{x}_T + \nu\bar{x}_A + \phi) \end{bmatrix}.$$

Proposition 6. *The unique equilibrium of* (5)–(7) *is locally stable.*

Proof. Let $p(s) = \det(sI - J_I) = p_3 s^3 + p_2 s^2 + p_1 s + p_0$ be the characteristic polynomial of the linearized system. The polynomial is:

$$p(s) = \det \begin{bmatrix} s + (a+b) & -c & d \\ \kappa - a & s + (\kappa + c + n) & m \\ b & n & s + (d + m + \phi) \end{bmatrix}.$$

We have $p_3 = 1$, $p_2 = a + b + c + d + n + m + \phi + \kappa$,

$$p_1 = \det \begin{bmatrix} -(a+b) & c \\ a - \kappa & -(\kappa + c + n) \end{bmatrix} + \det \begin{bmatrix} -(a+b) & -d \\ -b & -(d + m + \phi) \end{bmatrix} + \det \begin{bmatrix} -(\kappa + c + n) & -m \\ -n & -(d + m + \phi) \end{bmatrix},$$

and finally $p_0 = \det(-J_I)$. Some simple and tedious computations show that $p_k > 0$, $k = 0, 1, 2, 3$. This is necessary, yet not sufficient for stability. According to the Routh–Hurwitz criterion, a polynomial has roots with negative real part if and only if the elements of the first column of the Routh–Hurwitz table are positive. Such a table is:

$$\begin{array}{cc} p_3 & p_1 \\ p_2 & p_0 \\ \frac{p_2 p_1 - p_0 p_3}{p_2} & 0 \\ p_0 & 0 \end{array}$$

Then $p_3 = 1 > 0$, $p_2 > 0$ and $p_0 > 0$. It can be verified analytically that also $p_2 p_1 - p_0 p_3 > 0$, for all positive values of the coefficients. □

1.1.3 Parameter sensitivity

We numerically solved the ODEs describing the behavior of the inhibited module when each reaction rate is varied in a range. ODEs were integrated using MATLAB `ode23s` routine. The results are shown in Fig. S1.

1.2 Analysis of the activated module

1.2.1 Analysis in the absence of direct titration reaction

We recall the model for the activated module:

$$\dot{x}_T = \alpha(x_T^{tot} - x_T) r_A - \delta x_T x_I \quad (8)$$

$$\dot{x}_I = \kappa(x_I^{tot} - x_I - (x_T^{tot} - x_T)) - \delta x_T x_I \quad (9)$$

$$\dot{r}_A = \beta u_A - \alpha(x_T^{tot} - x_T) r_A - \phi r_A \quad (10)$$

Assumption 3. *We assume that* $x_I^{tot} \geq x_T^{tot}$.

Additionally, we make an assumption that relates parameters κ, δ, and the total concentrations of target and constitutive inhibitor.

Assumption 4. *We assume that* $x_I^{tot} - x_T^{tot} - \frac{\kappa}{\delta} \geq 0$.

Proposition 7. *For a given concentration of activator source* $\bar{u}_A$*, system* (8)–(10) *has unique equilibrium values* $\bar{x}_T$*,* $\bar{x}_I$ *and* $\bar{r}_A$*. The equilibrium* $\bar{x}_T$ *is a monotonic, strictly increasing function of* $\bar{u}_A$*.*

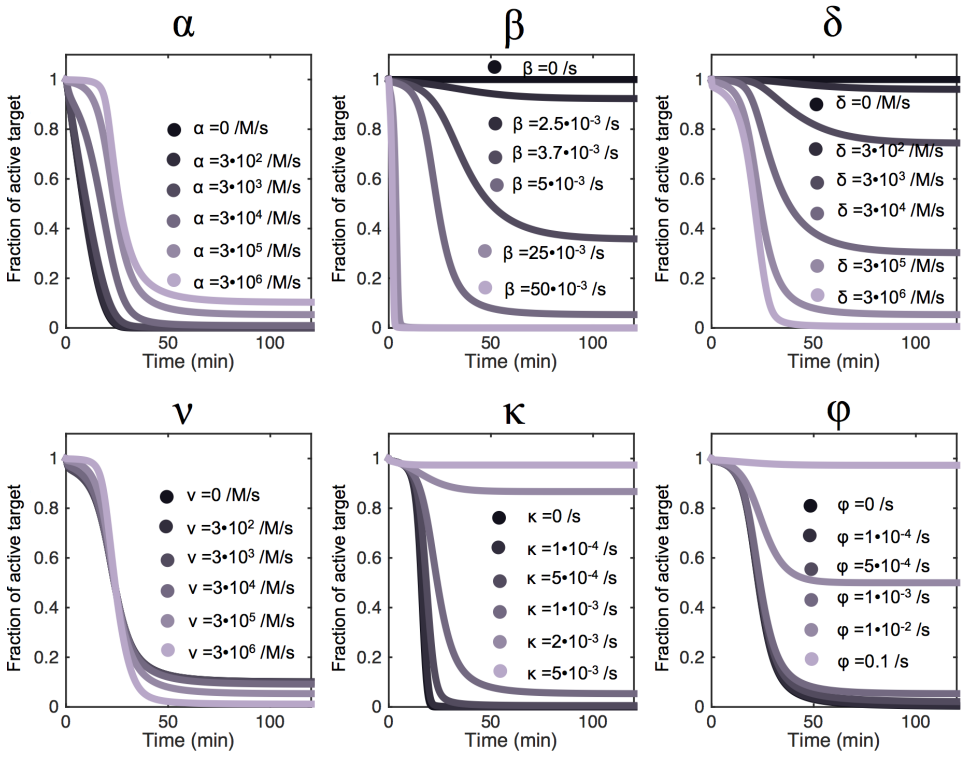

Figure S1: Numerical simulation showing the dependence of the normalized target concentration of the inhibited module ($x_T(t)/x_T^{tot}$) when the reaction rates are varied.

Proof. We begin by finding an expression for $\bar{x}_I$ as a function of $\bar{x}_T$. From $\dot{x}_I = 0$, we obtain:

$$\bar{x}_I(\bar{x}_T) = \frac{\kappa(x_I^{tot} - (x_T^{tot} - \bar{x}_T))}{\delta\bar{x}_T + \kappa}.$$

The equilibrium $\bar{x}_I$ is a monotonic decreasing function of $\bar{x}_T$, as can be seen by checking the sign of the partial derivative:

$$\frac{\partial\bar{x}_I}{\partial\bar{x}_T} = -\frac{\delta}{\kappa}\frac{x_I^{tot} - x_T^{tot} - \frac{\kappa}{\delta}}{(\frac{\delta}{\kappa}\bar{x}_T + 1)^2} \leq 0,$$

in view of Assumption 4.

We continue by finding $\bar{r}_A$ as a function of $\bar{x}_T$. From $\dot{x}_T = 0$, we obtain:

$$\bar{r}_A(\bar{x}_T) = \frac{\delta\bar{x}_T}{\alpha(x_T^{tot} - \bar{x}_T)}\bar{x}_I(\bar{x}_T).$$

With the same approach followed in the proof of Proposition 1, we can show that the equilibrium $\bar{r}_A$ is a monotonic, strictly increasing function of $\bar{x}_T$. Finally, from $\dot{r}_A = 0$ we find:

$$\bar{u}_A = \frac{1}{\beta}\left(\alpha(x_T^{tot} - \bar{x}_T) + \phi\right)\bar{r}_A(\bar{x}_T) = \frac{1}{\beta}(\delta\bar{x}_T\bar{x}_I(\bar{x}_T) + \phi\bar{r}_A(\bar{x}_T)) \doteq w(\bar{x}_T).$$

To identify structural trends between $\bar{u}_A$ and $\bar{x}_T$, we check the sign of the partial derivative $\partial(\bar{x}_T\bar{x}_I(\bar{x}_T))/\partial\bar{x}_T$; some tedious computations show that this partial derivative is always strictly positive, except for $\bar{x}_T = 0$. Therefore $w(\bar{x}_T)$ is a monotonic, strictly increasing function of $\bar{x}_T$; its inverse $\bar{x}_T \doteq k(\bar{u}_I) = w^{-1}(\bar{u}_I)$ is thus also a strictly increasing function. We conclude that the equilibrium $\bar{x}_T$ for a given $\bar{u}_A$ is unique, and so are the other equilibria $\bar{x}_I$ and $\bar{r}_A$. In particular, the higher the concentration of input U_A, the smaller the equilibrium concentration of X_T. □

Proposition 8. *The set*

$$0 \leq x_T \leq x_T^{tot}, \qquad \frac{\kappa}{\delta} \leq x_I \leq x_I^{tot}, \qquad r_A \geq 0 \tag{11}$$

is positively invariant [3] for (8)–(10)*.*

Proof. Since all the variables are non–negative and the variables x_T and x_I cannot exceed their total values, all the constraints are obvious with the exception of $\kappa/\delta \leq x_I$. We show that this constraint cannot be violated: if we start with $x_I(0) \geq \kappa/\delta$, then the constraint is satisfied for all $t > 0$. In fact, due to Assumption 4, for $x_I = \kappa/\delta$ we have

$$\dot{x}_I = \kappa(x_I^{tot} - \frac{\kappa}{\delta} - x_T^{tot} + x_T) - \delta x_T\frac{\kappa}{\delta} = \kappa(x_I^{tot} - x_T^{tot} - \frac{\kappa}{\delta}) \geq 0.$$

□

Proposition 9. *The solutions of system* (8)–(10) *are bounded.*

Proof. Species x_T and x_I are bounded by assumption. The dynamics of the regulator satisfies the inequality $\dot{r}_A(t) \leq \beta u_A^{max} - \phi r_A$. In view of the comparison principle, $r_A(t) \leq r_A(0)e^{-\phi t} + u_A^{max}\beta(1 - e^{-\phi t})/\phi$, which ensures $r_A(t) \leq \max\{r_A(0), u_A^{max}\beta/\phi\}$ at any point in time. □

Proposition 10. *The unique equilibrium of system* (8)–(10) *is locally stable.*

Proof. We follow the proof of Proposition 4. The Jacobian matrix is

$$J_A = \begin{bmatrix} -(\alpha\bar{r}_A + \delta\bar{x}_I) & -\delta x_T & \alpha(x_T^{tot} - \bar{x}_T) \\ \kappa - \delta\bar{x}_I & -(\kappa + \delta\bar{x}_T) & 0 \\ \alpha\bar{r}_A & 0 & -\alpha(x_T^{tot} - \bar{x}_T) - \phi \end{bmatrix}$$

and, since $\delta\bar{x}_I - \kappa > 0$ (Proposition 8), it can be recast as a Metzler matrix by changing sign to its second row and column. As can be shown by direct computation, all the coefficients of the characteristic polynomial $\det(\lambda I - J_A)$ are positive. □

1.2.2 Analysis in the presence of direct titration reactions

When titration reactions are present, the model becomes:

$$\dot{x}_T = \alpha(x_T^{tot} - x_T)r_A - \delta x_T x_I \quad (12)$$
$$\dot{x}_I = \kappa(x_I^{tot} - x_I - (x_T^{tot} - x_T)) - \delta x_T x_I - \nu x_I r_A \quad (13)$$
$$\dot{r}_A = \beta u_A - \alpha(x_T^{tot} - x_T)r_A - \phi r_A - \nu x_I r_A \quad (14)$$

Proposition 11. *The solutions of system* (12)–(14) *are globally bounded.*

Proof. Analogous to that of Proposition 5. □

Equilibria: First we find an expression for $\bar{x}_I$ as a function of $\bar{x}_T$. From $\dot{x}_T - \dot{x}_I = 0$, we obtain:

$$\kappa(x_I^{tot} - \bar{x}_I - (x_T^{tot} - \bar{x}_T)) = (\alpha(x_T^{tot} - \bar{x}_T) + \nu\bar{x}_I)\bar{r}_A,$$

and from $\dot{x}_T = 0$,

$$\alpha(x_T^{tot} - \bar{x}_T)\bar{r}_A = \delta\bar{x}_T\bar{x}_I.$$

Then

$$\bar{r}_A = \frac{\kappa(x_I^{tot} - \bar{x}_I - (x_T^{tot} - \bar{x}_T))}{\alpha(x_T^{tot} - \bar{x}_T) + \nu\bar{x}_I} = \frac{\delta\bar{x}_T\bar{x}_I}{\alpha(x_T^{tot} - \bar{x}_T)}$$

and we obtain a second order polynomial of the following form: $a_x\bar{x}_I^2 + b_x\bar{x}_I + c_x = 0$, where

$$a_x = \frac{\delta\nu\bar{x}_T}{\alpha(x_T^{tot} - \bar{x}_T)}, \quad b_x = \alpha\bar{x}_T + \kappa, \quad c_x = -\kappa(x_I^{tot} - (x_T^{tot} - \bar{x}_T)).$$

Since c_x is always negative, the unique positive and acceptable solution is

$$\bar{x}_I(\bar{x}_T) = \frac{-b_x + \sqrt{b_x^2 - 4a_x c_x}}{2a_x}.$$

Then, we find $\bar{r}_A$ as a function of $\bar{x}_T$. From $\dot{x}_T = 0$, we obtain:

$$\bar{r}_A(\bar{x}_T) = \frac{\delta\bar{x}_T\bar{x}_I(\bar{x}_T)}{\alpha(x_T^{tot} - \bar{x}_T)}.$$

Finally from $\dot{r}_A = 0$:

$$\bar{u}_A = \frac{1}{\beta}(\alpha(x_T^{tot} - \bar{x}_T) + \phi + \nu\bar{x}_I(\bar{x}_T))\bar{r}_A(\bar{x}_T).$$

Jacobian analysis: The Jacobian matrix is now:

$$J_A = \begin{bmatrix} -(\alpha\bar{r}_A + \delta\bar{x}_I) & -\delta\bar{x}_T & \alpha(x_T^{tot} - \bar{x}_T) \\ \kappa - \delta\bar{x}_I & -(\kappa + \delta\bar{x}_T + \nu\bar{r}_A) & -\nu\bar{x}_I \\ \alpha\bar{r}_A & -\nu\bar{r}_A & -(\alpha(x_T^{tot} - \bar{x}_T) + \nu\bar{x}_I + \phi) \end{bmatrix}$$

Proposition 12. *The unique equilibrium of* (12)–(14) *is locally stable.*

Proof. Analogous to that of Proposition 6. □

1.2.3 Parameter sensitivity

Fig. S2 shows the behavior of the activated module when each reaction rates is varied in a range. ODEs were integrated using MATLAB `ode23s` routine.

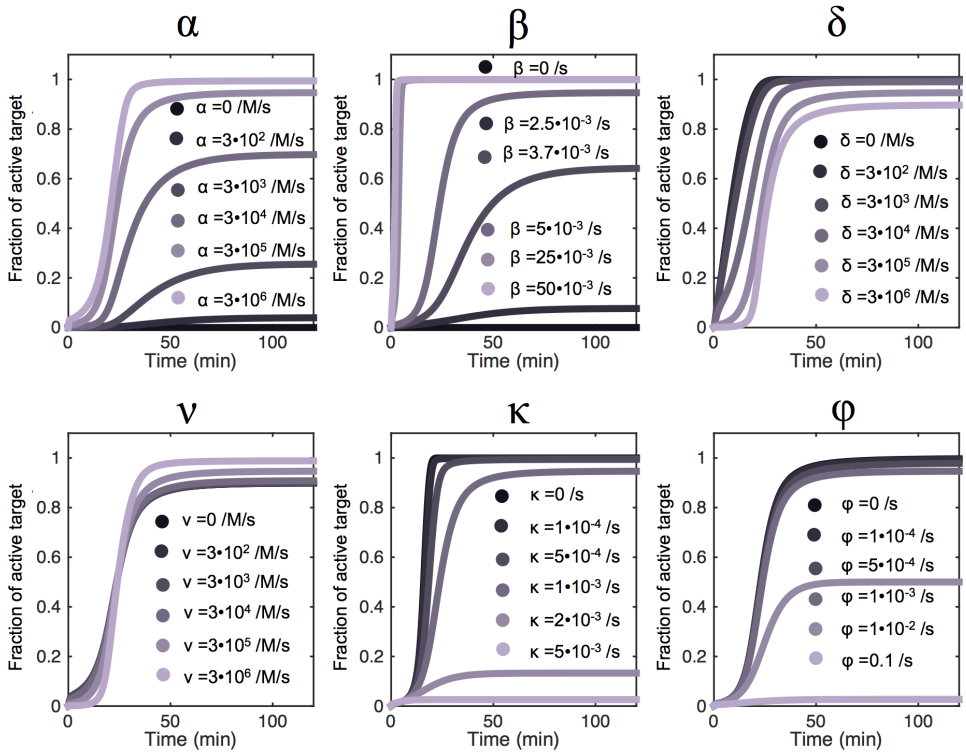

Figure S2: Numerical simulation showing the dependence of the normalized target concentration of the activated module ($x_T(t)/x_T^{tot}$) when the reaction rates are varied.

2 Oscillator

As discussed in the main text, we build an oscillator via the feedback interconnection of an inhibited module and an activated module. The reactions occurring in the system are:

	Activated subsystem	**Inhibited subsystem**
Activation:	$X_{R,A} + Z_T^* \xrightarrow{\alpha_z} Z_T + Z_I^*$	$X_A + X_T^* \xrightarrow{\alpha_x} X_T$
Output production:	$Z_T \xrightarrow{\beta_z} Z_{R,I} + Z_T$	$X_T \xrightarrow{\beta_x} X_{R,A} + X_T$
Inhibition:	$Z_T + Z_I \xrightarrow{\delta_z} Z_T^*$	$Z_{R,I} + X_T \xrightarrow{\delta_x} X_T^* + X_A^*$
Conversion:	$Z_I^* \xrightarrow{\kappa_z} Z_I$	$X_A^* \xrightarrow{\kappa_x} X_A$
Direct titration:	$X_{R,A} + Z_I \xrightarrow{\nu_z} Z_I^*$	$Z_{R,I} + X_A \xrightarrow{\nu_x} X_A^*$.
Degradation:	$Z_{R,I} \xrightarrow{\phi_z} 0$	$X_{R,A} \xrightarrow{\phi_x} 0$

The regulators interconnecting the modules are $x_{R,A}$, which is the output of the inhibited module and works as an activator for the activated module, and $z_{R,I}$, which is the output of the activated module and works as an inhibitor for the inhibited module. We recall that we assume mass conservation for species Z_T, Z_I, X_T, and X_A: $z_T^{tot} = z_T + z_T^*$, $z_I^{tot} = z_I + z_I^* + z_T^*$, $x_T^{tot} = x_T + x_T^*$, $x_A^{tot} = x_A + x_A^* + x_T$. Using the law of mass action we derive the differential equations:

$$\dot{z}_T = \alpha_z(z_T^{tot} - z_T)x_{R,A} - \delta_z z_T\, z_I, \tag{15}$$
$$\dot{z}_I = \kappa_z(z_I^{tot} - z_I - (z_T^{tot} - z_T)) - \delta_z z_T\, z_I - \nu_z x_{R,A}\, z_I, \tag{16}$$
$$\dot{x}_{R,A} = \beta_x x_T - \alpha_z(z_T^{tot} - z_T)\, x_{R,A} - \nu_z x_{R,A}\, z_I - \phi_x x_{R,A}, \tag{17}$$
$$\dot{x}_T = \alpha_x(x_T^{tot} - x_T)x_A - \delta_x x_T\, z_{R,I}, \tag{18}$$
$$\dot{x}_A = \kappa_x(x_A^{tot} - x_A - x_T) - \alpha_x(x_T^{tot} - x_T)\, x_A - \nu_x x_A\, z_{R,I}, \tag{19}$$
$$\dot{z}_{R,I} = \beta_z z_T - \delta_x x_T\, z_{R,I} - \nu_x x_A\, z_{R,I} - \phi_z z_{R,I}. \tag{20}$$

Throughout our analysis, we assume that $z_I^{tot} \geq z_T^{tot}$ and $x_A^{tot} \geq x_T^{tot}$.

As a preliminary result, we notice that the interconnection does not change the boundedness property of the solution.

Proposition 13. *The solutions of system* (15)–(20) *are bounded.*

Proof. The proposition follows from the fact that each subsystem has bounded solution for bounded inputs. Then we notice that the inhibited subsystem (x_T–x_A–$z_{R,I}$) has input $\beta_z z_T \leq \beta_z z_T^{tot}$, which is bounded, while the activated subsystem (z_T–z_I–$x_{R,A}$) has input $\beta_x x_T \leq \beta_x x_T^{tot}$, bounded as well. □

2.1 Analysis in the absence of direct titration reactions

2.1.1 Equilibrium conditions

In this section, we consider the oscillatory system (15)–(20) in the absence of titration reactions, *i.e.*, with $\nu_x = \nu_z = 0$. We derive equilibrium conditions that are consistent with those derived for the inhibited and activated module. First, we find an expression for $\bar{x}_T$ as a function of $\bar{z}_T$. From $\dot{z}_I = 0$, we obtain:

$$\bar{z}_I(\bar{z}_T) = \frac{\kappa_z(z_I^{tot} - (z_T^{tot} - \bar{z}_T))}{\delta_z \bar{z}_T + \kappa_z}.$$

From $\dot{z}_T = 0$, we obtain:

$$\bar{x}_{R,A}(\bar{z}_T) = \frac{\delta_z \bar{z}_T\, \bar{z}_I(\bar{z}_T)}{\alpha_z(z_T^{tot} - \bar{z}_T)}.$$

From $\dot{x}_{R,A} = 0$,

$$\bar{x}_T = \frac{1}{\beta_x}(\alpha_z(z_T^{tot} - \bar{z}_T) + \phi_x)\bar{x}_{R,A}(\bar{z}_T) \doteq w(\bar{z}_T).$$

As shown in Proposition 1, $\bar{x}_T$ is a monotonically decreasing function of $\bar{z}_T$.

We now find an expression for $\bar{z}_T$ as a function of $\bar{x}_T$. From $\dot{x}_A = 0$, we obtain:

$$\bar{x}_A(\bar{x}_T) = \frac{\kappa_x(x_A^{tot} - \bar{x}_T)}{\alpha_x(x_T^{tot} - \bar{x}_T) + \kappa_x}.$$

From $\dot{x}_T = 0$, we obtain:

$$\bar{z}_{R,I}(\bar{x}_T) = \frac{\alpha_x(x_T^{tot} - \bar{x}_T)\bar{x}_A(\bar{x}_T)}{\delta_x \bar{x}_T}.$$

From $\dot{z}_{R,I} = 0$,

$$\bar{z}_T = \frac{1}{\beta_z}(\delta_x \bar{x}_T + \phi_z)\bar{z}_{R,I}(\bar{x}_T) \doteq h(\bar{x}_T).$$

As shown in Proposition 7, $\bar{z}_T$ is a monotonically increasing function of $\bar{x}_T$. The functions $h(\bar{x}_T)$ and $w(\bar{z}_T)$ found above, because of their opposite trend, can admit a single intersection in the plane $(\bar{x}_T, \bar{z}_T)$. These equilibrium conditions will be used to find numerically or graphically the unique equilibrium point of the system.

2.1.2 Structural oscillations

The equilibrium conditions derived earlier show that there exists a single equilibrium, around which we linearize the system. It is convenient to change the sign of some of the variables: $-z_I$, $-x_T$, $-x_A$. The Jacobian matrix of system (15)–(20) with $\nu_z = \nu_x = 0$ becomes:

$$J = \left[\begin{array}{ccc|ccc} -\alpha_z\bar{x}_{R,A} - \delta_z\bar{z}_I & \delta_z\bar{z}_T & \alpha_z(z_T^{tot} - \bar{z}_T) & 0 & 0 & 0 \\ -\kappa_z + \delta_z\bar{z}_I & -\kappa_z - \delta_z\bar{z}_T & 0 & 0 & 0 & 0 \\ \alpha_z\bar{x}_{R,A} & 0 & -\alpha_z(z_T^{tot} - \bar{z}_T) - \phi_x & 0 & -\beta_x & 0 \\ \hline \beta_z & 0 & 0 & -\delta_x\bar{x}_T - \phi_z & \delta_x\bar{z}_{R,I} & 0 \\ 0 & 0 & 0 & \delta_x\bar{x}_T & -\alpha_x\bar{x}_A - \delta_x\bar{z}_{R,I} & \alpha_x(x_T^{tot} - \bar{x}_T) \\ 0 & 0 & 0 & 0 & -\kappa_x + \alpha_x\bar{x}_A & -\kappa_x - \alpha_x(x_T^{tot} - \bar{x}_T) \end{array}\right] \tag{21}$$

We call *strong candidate oscillator* [1, 2] a system which can be locally unstable exclusively due to the existence of complex conjugate eigenvalues with nonnegative real part (in other words, the system does not admit real nonnegative eigenvalues).

Proposition 14. *Under Assumptions 1, 2, 3, and 4, system* (15)–(20) *is a strong candidate oscillator.*

Proof. The computation of the characteristic polynomial $\det(\lambda I - J)$ reveals that all the coefficients are positive (note that we assume $-\kappa_z + \delta_z\bar{z}_I > 0$ and $-\kappa_x + \alpha_x\bar{x}_A > 0$). A polynomial with positive coefficients cannot have nonnegative real roots. □

2.1.3 Linear analysis

The Jacobian (21) clearly shows that the system is the feedback interconnection of two subsystems of the third order. To simplify the notation we define:

$$\begin{array}{lcllcl} a_1 & \doteq & \delta_z\bar{z}_T, & a_2 & \doteq & \delta_x\bar{x}_T, \\ b_1 & \doteq & \delta_z\bar{z}_I, & b_2 & \doteq & \delta_x\bar{z}_{R,I}, \\ c_1 & \doteq & \alpha_z\bar{x}_{R,A}, & c_2 & \doteq & \alpha_x\bar{x}_A, \\ d_1 & \doteq & \alpha_z(z_T^{tot} - \bar{z}_T), & d_2 & \doteq & \alpha_x(x_T^{tot} - \bar{x}_T), \\ e_1 & \doteq & \kappa_z, & e_2 & \doteq & \kappa_x, \\ h_1 & \doteq & \phi_x, & h_2 & \doteq & \phi_z, \end{array}$$

Then, defining vectors $\xi_1 = \begin{bmatrix} z_T & -z_I & x_{R,A} \end{bmatrix}^\top$ and $\xi_2 = \begin{bmatrix} z_{R,I} & -x_T & -x_A \end{bmatrix}^\top$, the linearized system can be rewritten as the feedback interconnection of:

$$\dot{\xi}_1 = A_1\xi_1 + \beta_x B_1\omega_2, \quad \omega_1 = C_1\xi_1,$$

and

$$\dot{\xi}_2 = A_2\xi_2 + \beta_z B_2\omega_1, \quad \omega_2 = C_2\xi_2,$$

where:

$$A_1 = \begin{bmatrix} -(c_1+b_1) & a_1 & d_1 \\ -e_1+b_1 & -(e_1+a_1) & 0 \\ c_1 & 0 & -(d_1+h_1) \end{bmatrix}, \quad B_1 = \begin{bmatrix} 0 \\ 0 \\ -1 \end{bmatrix}, \quad C_1 = \begin{bmatrix} 1 & 0 & 0 \end{bmatrix} \tag{22}$$

and

$$A_2 = \begin{bmatrix} -(a_2+h_2) & b_2 & 0 \\ a_2 & -(c_2+b_2) & d_2 \\ 0 & -e_2+c_2 & -(e_2+d_2) \end{bmatrix}, \quad B_2 = \begin{bmatrix} 1 \\ 0 \\ 0 \end{bmatrix}, \quad C_2 = \begin{bmatrix} 0 & 1 & 0 \end{bmatrix}. \tag{23}$$

By applying the Laplace transform method, we can obtain an input-output representation of the two subsystems in terms of their transfer functions[1]: $F_1(s) = -\frac{n_1(s)}{d_1(s)}$ and $F_2(s) = \frac{n_2(s)}{d_2(s)}$. Since the overall feedback loop is negative and all the coefficients of the numerator and denominator polynomials $n_1(s)$, $d_1(s)$, $n_2(s)$, $d_2(s)$ are positive, the closed–loop characteristic polynomial also has positive coefficients. Therefore it cannot admit non-negative real roots, as stated in the following proposition, hence the system is a strong candidate oscillator.

Proposition 15. *Consider system* (15)–(20)*, where $\nu_x = \nu_z = 0$, linearized around its only equlibrium point. Its characteristic polynomial has no real nonnegative roots. If instability occurs, it is oscillatory, namely due to complex roots with positive real part.*

The fact that the system is a candidate oscillator in the strong sense does not mean that the system oscillates for any choice of the parameters. In fact, numerical simulations show that oscillations occur only in a limited region in the plane defined by β_z and β_x.

It is worth noticing that in the absence of titration reactions, being $c_2 - e_2$ and $b_1 - e_1$ positive quantities, the system is the negative feedback interconnection of two monotone subsystems, associated with the modules (see [1, 2] and the references therein): this structurally explains its oscillatory nature.

2.2 Analysis in the presence of direct titration reactions

2.2.1 Equilibrium conditions

We consider in this section the oscillatory system (15)–(20) in the presence of non–zero ν_x and ν_z. We begin by finding two expressions of $\bar{x}_{R,A}$ as a function of the other variables. This can be done by setting $\dot{z}_T - \dot{z}_I = 0$ and $\dot{z}_T = 0$. Then, we equate the two expressions for $\bar{x}_{R,A}$ and we achieve:

$$\frac{\delta_z \bar{z}_T\, \bar{z}_I}{\alpha_z(z_T^{tot} - \bar{z}_T)} = \frac{\kappa_z(z_I^{tot} - \bar{z}_I - (z_T^{tot} - \bar{z}_T))}{\alpha_z(z_T^{tot} - \bar{z}_T) + \nu_z \bar{z}_I},$$

[1]Given a linear system with an input $u(t)$ and an output $y(t)$, its transfer function $F(s)$ is the ratio between the Laplace transform of the output and the Laplace transform of the input: $F(s) = \frac{Y(s)}{U(s)}$.

which defines a relationship between $\bar{z}_T$ and $\bar{z}_I$ at steady state. The equilibrium $\bar{z}_I$ can thus be derived as the solution of the second order equation $a_z\bar{z}_I^2 + b_z\bar{z}_I + c_z = 0$, where $a_z = \left(\frac{\delta_z\nu_z}{\alpha_z}\right)\frac{\bar{z}_T}{z_T^{tot}-\bar{z}_T}$, $\quad b_z = (\delta_z\bar{z}_T + \kappa_z)$ and $c_z = -\kappa_z(z_I^{tot} - (z_T^{tot} - \bar{z}_T))$. Assuming $z_I^{tot} > z_T^{tot}$, since $a_z c_z < 0$, the only admissible positive solution is:

$$\bar{z}_I(\bar{z}_T) = \frac{-b_z + \sqrt{b_z^2 - 4a_z c_z}}{2a_z}.$$

Then,

$$\bar{x}_{R,A} = \frac{\delta_z\bar{z}_T\,\bar{z}_I(\bar{z}_T)}{\alpha_z(z_T^{tot} - \bar{z}_T)}.$$

Finally, we can find $\bar{x}_T$ as a function of $\bar{z}_T$, by setting $\dot{x}_{R,A} = 0$:

$$\bar{x}_T = \frac{1}{\beta_x}(\alpha_z(z_T^{tot} - \bar{z}_T) + \phi_x + \nu_z\bar{z}_I(\bar{z}_T))\bar{x}_{R,A}(\bar{z}_T).$$

We can proceed similarly to derive $\bar{z}_T$ as a function of $\bar{x}_T$. Setting $\dot{x}_T + \dot{x}_A = 0$ and $\dot{x}_T = 0$, we find two different expressions for $\bar{z}_{R,I}$. Equating these expressions we find:

$$\frac{\alpha_x(x_T^{tot} - \bar{x}_T)\,\bar{x}_A}{\delta_x\bar{x}_T} = \frac{\kappa_x(x_A^{tot} - \bar{x}_A - \bar{x}_T)}{\delta_x\bar{x}_T + \nu_x\bar{x}_A,}$$

so we can isolate the relationship between $\bar{x}_T$ and $\bar{x}_A$ at steady state. As done before, we derive the equilibrium $\bar{x}_A$ as the solution of the second order equation $a_x\bar{x}_A^2 + b_x\bar{x}_A + c_x = 0$, where $a_x = \left(\frac{\alpha_x\nu_x}{\delta_x}\right)\frac{x_T^{tot}-\bar{x}_T}{\bar{x}_T}$, $b_x = \left(\alpha_x(x_T^{tot} - \bar{x}_T) + \kappa_x\right)$ and $c_x = -\kappa_x(x_A^{tot} - \bar{x}_T)$. Assuming $x_A^{tot} > x_T^{tot}$, since again $a_x c_x < 0$, the only admissible positive solution is:

$$\bar{x}_A(\bar{x}_T) = \frac{-b_x + \sqrt{b_x^2 - 4a_x c_x}}{2a_x}.$$

Then,

$$\bar{z}_{R,I} = \frac{\alpha_x(x_T^{tot} - \bar{x}_T)\,\bar{x}_A(\bar{x}_T)}{\delta_x\bar{x}_T}.$$

Finally, we can find $\bar{z}_T$ as a function of $\bar{x}_T$, by setting $\dot{z}_{R,I} = 0$:

$$\bar{z}_T = \frac{1}{\beta_z}(\delta_x\bar{x}_T + \phi_z + \nu_x\bar{x}_A(\bar{x}_T))\bar{z}_{R,I}(\bar{x}_T).$$

Once we find the only admissible equilibrium values $\bar{z}_T$, $\bar{z}_I$, $\bar{x}_T$ and $\bar{x}_A$ we can find $\bar{z}_{R,I}$ and $\bar{x}_{R,A}$.

$$\dot{z}_{R,I} = 0 \quad \Longrightarrow \quad \bar{z}_{R,I} = \frac{\beta_z\bar{z}_T}{\delta_x\bar{x}_T + \nu_x\bar{x}_A + \phi_z},$$
$$\dot{x}_{R,A} = 0 \quad \Longrightarrow \quad \bar{x}_{R,A} = \frac{\beta_x\bar{x}_T}{\alpha_z(z_T^{tot} - \bar{z}_T) + \nu_z\bar{z}_I + \phi_x}.$$

2.2.2 Structural oscillations

As done before, we change the sign to some of the variables, which become $-z_I$, $-x_T$, $-x_A$; the Jacobian of the system in the presence of titration reactions becomes matrix J_ν

$J_\nu =$ (24)

$$\left[\begin{array}{ccc|ccc}
-\alpha_z\bar{x}_{R,A} - \delta_z\bar{z}_I & \delta_z\bar{z}_T & \alpha_z(z_T^{tot} - \bar{z}_T) & 0 & 0 & 0 \\
-\kappa_z + \delta_z\bar{z}_I & -\kappa_z - \delta_z\bar{z}_T - \nu_z\bar{x}_{R,A} & \nu_z\bar{z}_I & 0 & 0 & 0 \\
\alpha_z\bar{x}_{R,A} & \nu_z\bar{x}_{R,A} & -\alpha_z(z_T^{tot} - \bar{z}_T) - \nu_z\bar{z}_I - \phi_x & 0 & -\beta_x & 0 \\
\hline
\beta_z & 0 & 0 & -\delta_x\bar{x}_T - \nu_x\bar{x}_A - \phi_z & \delta_x\bar{z}_{R,I} & \nu_x\bar{z}_{R,I} \\
0 & 0 & 0 & \delta_x\bar{x}_T & -\alpha_x\bar{x}_A - \delta_x\bar{z}_{R,I} & \alpha_x(x_T^{tot} - \bar{x}_T) \\
0 & 0 & 0 & \nu_x\bar{x}_A & -\kappa_x + \alpha_x\bar{x}_A & -\kappa_x - \alpha_x(x_T^{tot} - \bar{x}_T) - \nu_x\bar{z}_{R,I}
\end{array}\right]$$

2.2.3 Linear analysis

As done earlier, we simplify the notation defining:

$$\begin{array}{lcllcl} a_1 &\doteq& \delta_z \bar{z}_T, & a_2 &\doteq& \delta_x \bar{x}_T, \\ b_1 &\doteq& \delta_z \bar{z}_I, & b_2 &\doteq& \delta_x \bar{z}_{R,I}, \\ c_1 &\doteq& \alpha_z \bar{x}_{R,A}, & c_2 &\doteq& \alpha_x \bar{x}_A, \\ d_1 &\doteq& \alpha_z (z_T^{tot} - \bar{z}_T), & d_2 &\doteq& \alpha_x (x_T^{tot} - \bar{x}_T), \\ e_1 &\doteq& \kappa_z, & e_2 &\doteq& \kappa_x, \\ f_1 &\doteq& \nu_z \bar{x}_{R,A}, & f_2 &\doteq& \nu_x \bar{x}_A, \\ g_1 &\doteq& \nu_z \bar{z}_I, & g_2 &\doteq& \nu_x \bar{z}_{R,I}. \\ h_1 &\doteq& \phi_x, & h_2 &\doteq& \phi_z \end{array}$$

Then, defining $\xi_1 = \begin{bmatrix} z_T & -z_I & -x_{R,A} \end{bmatrix}^\top$ and $\xi_2 = \begin{bmatrix} z_{R,I} & -x_T & -x_A \end{bmatrix}^\top$, the linearized system can be rewritten as the feedback interconnection of two linear systems:

$$\dot{\xi}_1 = A_1 \xi_1 + \beta_x B_1 \omega_2, \quad \omega_1 = C_1 \xi_1,$$

and

$$\dot{\xi}_2 = A_2 \xi_2 + \beta_z B_2 \omega_1, \quad \omega_2 = C_2 \xi_2,$$

where:

$$A_1 = \begin{bmatrix} -(c_1 + b_1) & a_1 & d_1 \\ -e_1 + b_1 & -(e_1 + a_1 + f_1) & g_1 \\ c_1 & f_1 & -(d_1 + g_1 + h_1) \end{bmatrix}, \quad B_1 = \begin{bmatrix} 0 \\ 0 \\ -1 \end{bmatrix}, \quad C_1 = \begin{bmatrix} 1 & 0 & 0 \end{bmatrix} \tag{25}$$

and

$$A_2 = \begin{bmatrix} -(a_2 + f_2 + h_2) & b_2 & g_2 \\ a_2 & -(c_2 + b_2) & d_2 \\ f_2 & -e_2 + c_2 & -(e_2 + d_2 + g_2) \end{bmatrix}, \quad B_2 = \begin{bmatrix} 1 \\ 0 \\ 0 \end{bmatrix}, \quad C_2 = \begin{bmatrix} 0 & 1 & 0 \end{bmatrix}. \tag{26}$$

The transfer functions associated with the two subsystems (25) and (26) are:

$$F_1(s) = -\frac{d_1 s + a_1 g_1 + d_1 e_1 + d_1 a_1 + d_1 f_1}{p_1(s)}$$

and

$$F_2(s) = \frac{a_2 s + a_2 e_2 + a_2 d_2 + a_2 g_2 + d_2 f_2}{p_2(s)},$$

where $p_1(s)$ and $p_2(s)$ are third order polynomials having positive coefficients.

As in the case without titration reactions, the interconnection of the two subsystems is a negative feedback loop. The polynomials of the numerator and denominator of both the transfer functions have positive coefficients. As a consequence, the closed–loop characteristic polynomial has positive coefficients. A polynomial with positive coefficients cannot have nonnegative real roots. Therefore, instability can occur only with complex conjugate poles with positive real part, thus it can only be oscillatory. This confirms the result of our previous structural analysis.

Proposition 16. *Consider system* (15)–(20)*, where* $\nu_x > 0$, $\nu_z > 0$*, linearized around its only equlibrium point. Its characteristic polynomial has no real nonnegative roots. Instability can only occur due to complex roots with positive real part.*

2.3 Numerical simulations

2.3.1 Randomized parameter search

Table S1: Nominal parameters for the oscillator model (15)–(20)

Rate	Value	Rate	Value
α_z (/M/s)	$75 \cdot 10^3$	α_x (/M/s)	$3 \cdot 10^5$
δ_z (/M/s)	$3 \cdot 10^5$	δ_x (/M/s)	$3 \cdot 10^5$
ν_z (/M/s)	$3 \cdot 10^5$	ν_x (/M/s)	$3 \cdot 10^5$
β_z (/s)	$5 \cdot 10^{-3}$	β_x (/s)	$2 \cdot 10^{-2}$
κ_z (/s)	$1 \cdot 10^{-3}$	κ_x (/s)	$1 \cdot 10^{-3}$
ϕ_z (/s)	$1 \cdot 10^{-3}$	ϕ_x (/s)	$1 \cdot 10^{-3}$
z_T^{tot} (nM)	250	x_T^{tot} (nM)	120
z_I^{tot} (nM)	700	x_A^{tot} (nM)	300

We numerically searched parameters that yield an oscillatory behavior in model (15)–(20). We generated random parameter values starting from the nominal parameter set listed on Table S1. We generated several hundreds of random parameter sets; reaction rates were varied in the range from 10^{-3} to 10^3 times their nominal values; z_T^{tot}, z_I^{tot}, x_T^{tot} and x_A^{tot} were changed in the range from 10^{-1} to 10 times their nominal values . For each parameter set, the differential equations (15)–(20) are solved using the deterministic integrator RADAU, included in the software PyDSTool [4]. A parameter set is classified as "oscillatory" if at least 3 oscillations are detected, their average period is beween $0.5h$ and $10h$, and their average amplitude is larger than 10 nM. Each trajectory was integrated to have a duration of 20 h. Our method follows the approach proposed in [5].

Period and amplitude were computed by identifying minima and maxima of oscillations, as shown in the inset of Fig. S3. For each three consecutive points of a trajectory, we define $d1$ and $d2$ as shown in Fig. S3 B: $d1 = p_n - p_{n-1}$ and $d2 = p_n - p_{n+1}$. If the product $d1 \cdot d2$ is positive and $d1$ is positive, then p_n is classified as a local maximum; if $d1$ is negative, then p_n is classified as a local minimum. Period and amplitude are computed from the identified maxima and minima, as sketched in Fig. S3 C. Period and amplitude are averaged over all the different measured peaks and wells and compared to the aforementioned thresholds.

Fig. S3 A shows the correlations among pairs of parameters that yield oscillations in the absence of direct titration reactions. Fig. S4 shows the results in the presence of titration reactions: the probability of oscillation is significantly increased. Some of the correlation plots show clear patterns. For example the plots clearly show that z_I^{tot} should be larger than z_T^{tot} and x_A^{tot} larger than x_T^{tot}. Both β_z and β_x should be sufficiently large (relative to the nominal value).

2.3.2 Classification of dynamic behaviors in a region of the parameter space

We now classify equilibria as oscillatory or not by checking the eigenvalues of the Jacobian matrix (24) for a given parameter set (we recall that the system has a unique equilibrium for arbitrary choices of parameters). Starting from the nominal parameters listed in Table S1; all parameters were changed in the range from 10^{-1} to 10 times their nominal values. Two parameters were varied at a time, while others were held constant, to generate each subplot of Fig. S5 and S6. Equilibria were computed as the intersections of the analytical equilibrium expressions found at Section 2.2.1. Then, the stability properties of the equilibrium points are computed by finding the eigenvalues of the Jacobian evaluated at the equilibrium. When the Jacobian has at least one pair of complex conjugate eigenvalues with positive real part, it is classified as oscillatory; otherwise, it is classified as non-oscillatory and thus stable.

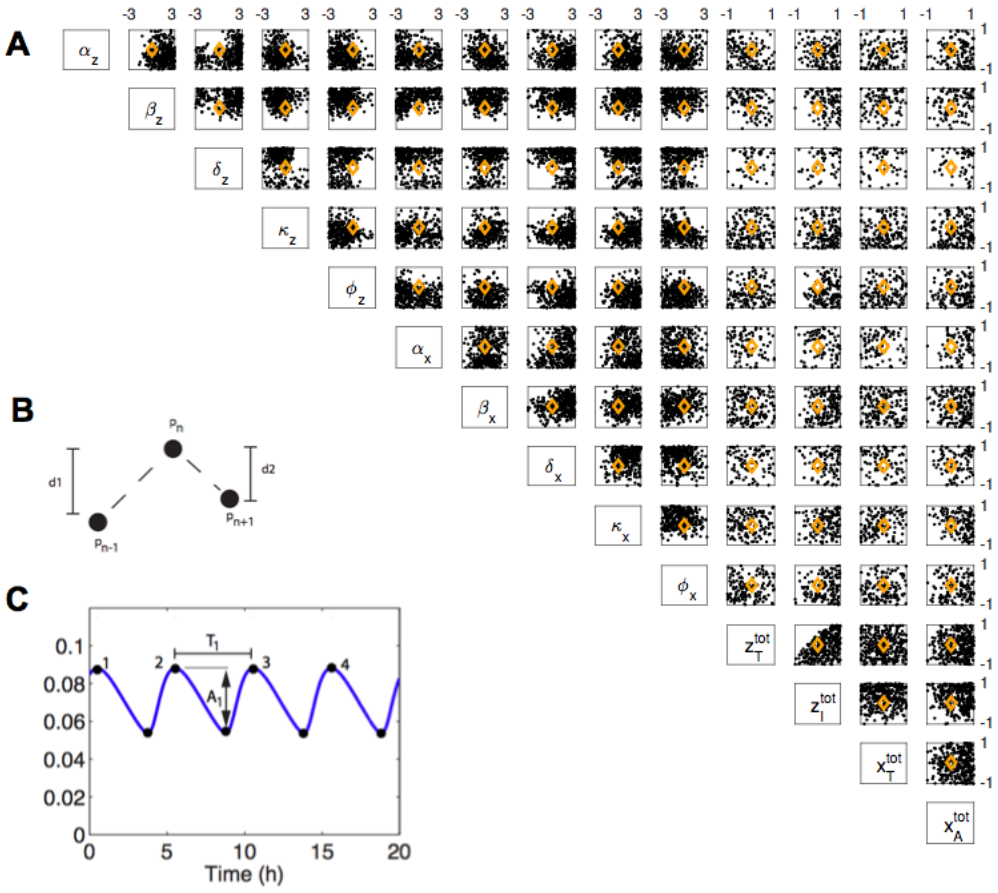

Figure S3: A: Absence of direct titration reactions. Correlation between randomly chosen parameters that yield oscillatory behavior. B: Points required for the identification of period and amplitude. C: Period and amplitude were measured as shown here and averaged over the trajectory.

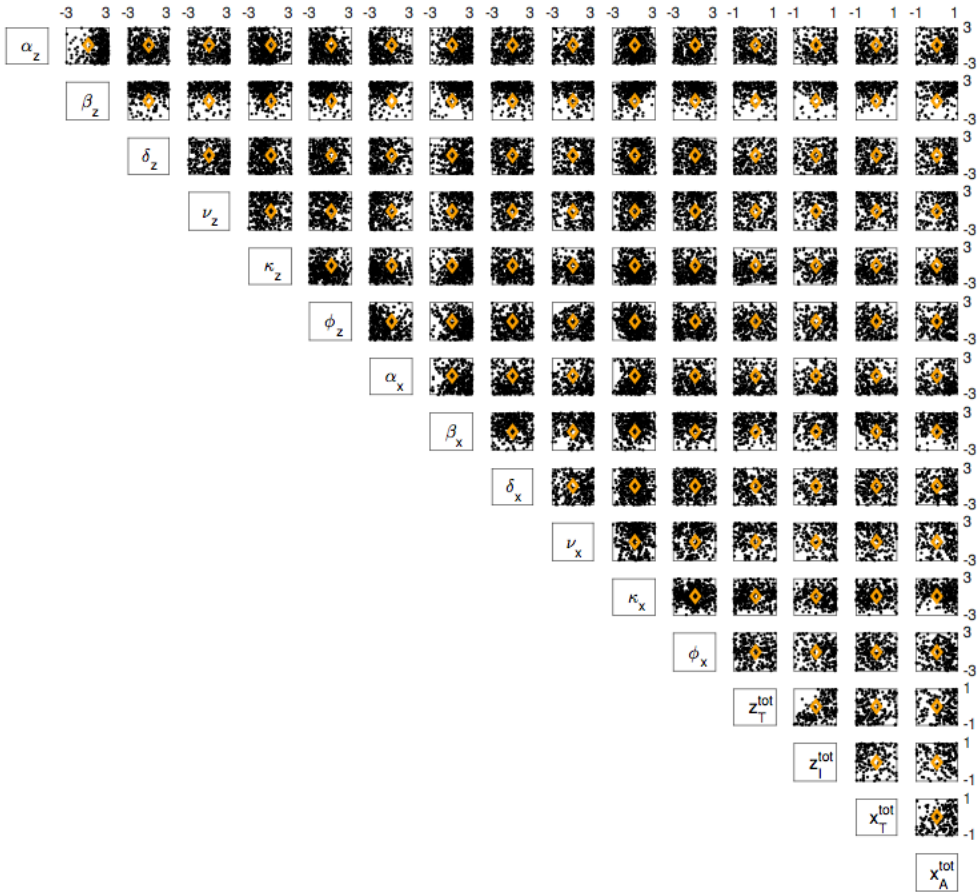

Figure S4: Presence of direct titration reactions. Correlation between randomly chosen parameters that yield oscillatory behavior. The probability of oscillation for a randomly chosen set of parameters significantly increases relative to Fig. S3.

We summarize our results in Fig. S5 and S6, which show the influence of the parameters on the stability properties of the unique equilibrium of the system; we consider the case where titration reactions are absent (Fig. S5), and the case where titration reactions are comparable to the inhibition/activation rates of the regulators that interconnect the two modules (Fig. S6). The classification is color coded as follows: points where at least one pair of eigenvalues is complex with positive real part are shown in orange color; points at which we find real and negative eigenvalues or complex with negative real part are shown in blue color. These plots show some linear correlations among parameters that yield oscillations: (β_z, x_A^{tot}) and (β_x, z_I^{tot}) are positively correlated; (κ_x, x_A^{tot}) and (κ_z, x_I^{tot}) are negatively correlated in order to guarantee an oscillatory behavior. The presence of titration reactions considerably expands the oscillatory regions for all pairs of parameters.

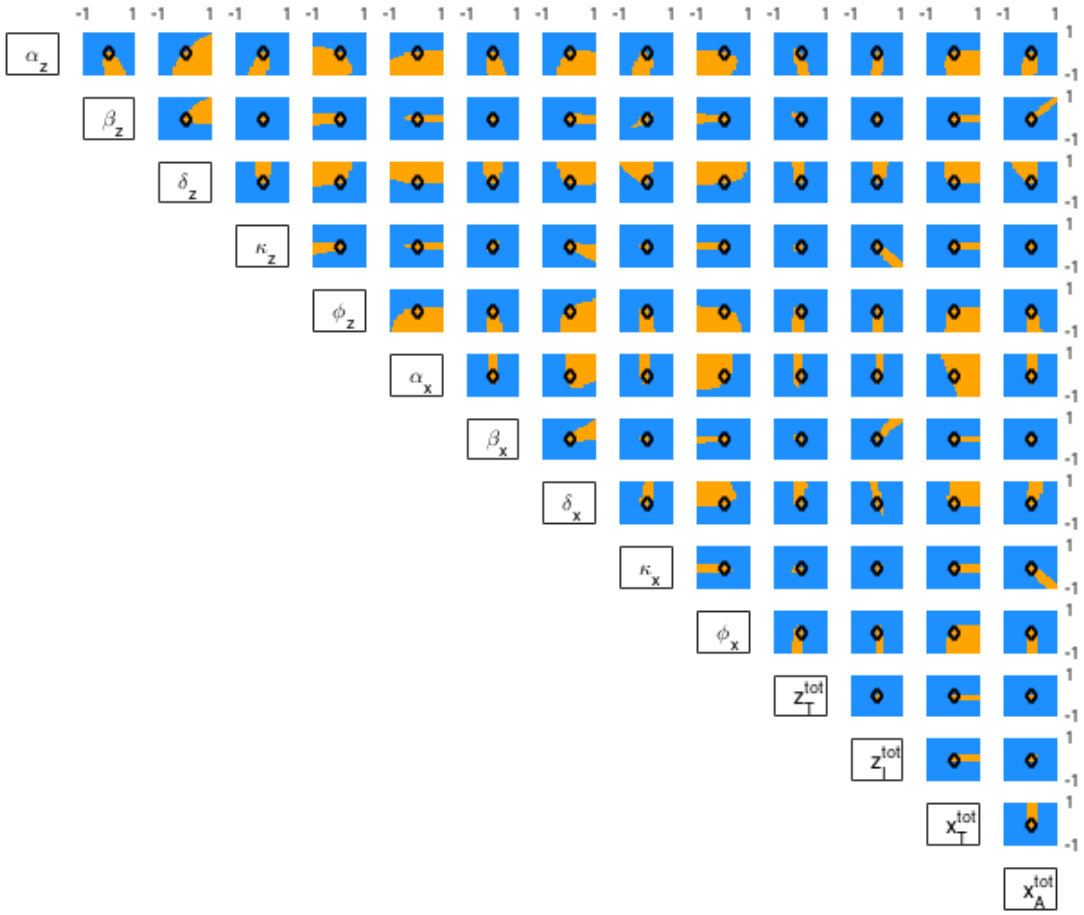

Figure S5: Absence of direct titration reactions: the log plots show the influence of variations of parameters on the stability of the equilibrium. Each parameter was varied between one tenth to ten times the nominal value (black diamond). Orange regions are oscillatory; blue regions indicate stable equilibria.

Figure S6: Presence of direct titration reactions: the log plots show the influence of variations of parameters on the stability of the equilibrium. Each parameter was varied between one tenth to ten times the nominal value (black diamond). Orange regions are oscillatory; blue regions indicate stable equilibria. The orange (oscillatory) regions are considerably larger than those in Fig. S5, where titration is absent.

3 Bistable system

We build a bistable system via the feedback interconnection of two inhibited modules. The reactions describing the bistable system are:

	Subsystem 1	**Subsystem 2**
Activation:	$Z_A + Z_T^* \xrightarrow{\alpha_z} Z_T$	$X_A + X_T^* \xrightarrow{\alpha_x} X_T$
Output production:	$Z_T \xrightarrow{\beta_z} Z_{R,I} + Z_T$	$X_T \xrightarrow{\beta_x} X_{R,I} + X_T$
Inhibition:	$X_{R,I} + Z_T \xrightarrow{\delta_z} Z_T^* + Z_A^*$	$Z_{R,I} + X_T \xrightarrow{\delta_x} X_T^* + X_A^*$
Direct titration:	$X_{R,I} + Z_A \xrightarrow{\nu_z} Z_A^*$	$Z_{R,I} + X_A \xrightarrow{\nu_x} X_A^*$
Conversion:	$Z_A^* \xrightarrow{\kappa_z} Z_A$	$X_A^* \xrightarrow{\kappa_x} X_A$
Degradation:	$Z_{R,I} \xrightarrow{\phi_z} 0$	$X_{R,I} \xrightarrow{\phi_x} 0$

The regulators interconnecting the modules are $x_{R,I}$ and $z_{R,I}$; both work as inhibitors. We assume mass conservation for species Z_T, Z_A, X_T, and X_A: $z_T^{tot} = z_T + z_T^*$, $z_A^{tot} = z_A + z_A^* + z_T$, $x_T^{tot} = x_T + x_T^*$, $x_A^{tot} = x_A + x_A^* + x_T$. The corresponding ODEs are:

$$\dot{z}_T = \alpha_z(z_T^{tot} - z_T)z_A - \delta_z z_T x_{R,I}, \tag{27}$$

$$\dot{z}_A = \kappa_z(z_A^{tot} - z_A - z_T) - \alpha_z(z_T^{tot} - z_T)z_A - \boxed{\nu_z x_{R,I} z_A}, \tag{28}$$

$$\dot{x}_{R,I} = \beta_x x_T - \delta_z z_T x_{R,I} - \phi_x x_{R,I} - \boxed{\nu_z x_{R,I} z_A}, \tag{29}$$

$$\dot{x}_T = \alpha_x(x_T^{tot} - x_T)x_A - \delta_x x_T z_{R,I}, \tag{30}$$

$$\dot{x}_A = \kappa_x(x_A^{tot} - x_A - x_T) - \alpha_x(x_T^{tot} - x_T)x_A - \boxed{\nu_x x_A z_{R,I}}, \tag{31}$$

$$\dot{z}_{R,I} = \beta_z z_T - \delta_x x_T z_{R,I} - \phi_z z_{R,I} - \boxed{\nu_x x_A z_{R,I}}. \tag{32}$$

Boxes highlight the terms corresponding to titration reactions. The two modules correspond to the subsystems z_T–z_A–$x_{R,I}$ and x_T–x_A–$z_{R,I}$.

Proposition 17. *The solutions of the two separated modules, as well as those of the interconnected system* (27)–(32)*, are globally bounded.*

Proof. Analogous to the proofs of Propositions 5, 11 and 13. □

3.1 Analysis in the absence of direct titration reactions

3.1.1 Equilibrium conditions

We consider system (27)–(32) in the absence of titration reactions, *i.e.*, with $\nu_x = \nu_z = 0$. We begin by setting equations $\dot{x}_T + \dot{x}_A = 0$ and we combine them with $\dot{x}_T = 0$. From here $\bar{z}_{R,I}$ is isolated as:

$$\bar{z}_{R,I} = \frac{\alpha_x(x_T^{tot} - \bar{x}_T)\,\bar{x}_A}{\delta_x \bar{x}_T} = \frac{\kappa_x(x_A^{tot} - \bar{x}_A - \bar{x}_T)}{\delta_x \bar{x}_T}.$$

We then find a relationship between $\bar{x}_T$ and $\bar{x}_A$ at steady state:

$$\bar{x}_A = \frac{\kappa_x(x_A^{tot} - \bar{x}_T)}{\alpha_x(x_T^{tot} - \bar{x}_T) + \kappa_x}.$$

Finally, setting equations $\dot{x}_T + \dot{x}_A = 0$ and $\dot{z}_{R,I} = 0$ we get:

$$\bar{z}_T = \frac{\kappa_x}{\beta_z}(x_A^{tot} - \bar{x}_A(\bar{x}_T) - \bar{x}_T) + \frac{\phi_z}{\beta_z}\bar{z}_{R,I}(\bar{x}_T). \tag{33}$$

The system is symmetric, so we now use the same procedure to obtain $\bar{x}_T(\bar{z}_T)$. We start setting $\dot{z}_T + \dot{z}_A = 0$ and equation $\dot{x}_{R,I} = 0$. We find:

$$\bar{x}_T = \frac{\kappa_z}{\beta_x}(z_A^{tot} - \bar{z}_A(\bar{z}_T) - \bar{z}_T) + \frac{\phi_x}{\beta_x}\bar{x}_{R,I}(\bar{z}_T). \tag{34}$$

Both equilibrium conditions are monotonically decreasing, which guarantees uniqueness of the equilibrium.

3.1.2 Structural bistability

The Jacobian matrix of system (27)–(32) with $\nu_x = \nu_z = 0$ is:

$$J_\nu = \begin{bmatrix} -\alpha_z\bar{z}_A - \delta_z\bar{x}_{R,I} & \alpha_z(z_T^{tot} - \bar{z}_T) & \delta_z\bar{z}_T & 0 & 0 & 0 \\ -\kappa_z + \alpha_z\bar{z}_A & -\kappa_z - \alpha_z(z_T^{tot} - \bar{z}_T) & 0 & 0 & 0 & 0 \\ \delta_z\bar{x}_{R,I} & 0 & -\delta_z\bar{z}_T - \phi_x & -\beta_x & 0 & 0 \\ 0 & 0 & 0 & -\alpha_x\bar{x}_A - \delta_x\bar{z}_{R,I} & \alpha_x(x_T^{tot} - \bar{x}_T) & \delta_x\bar{x}_T \\ 0 & 0 & 0 & -\kappa_x + \alpha_x\bar{x}_A & -\kappa_x - \alpha_x(x_T^{tot} - \bar{x}_T) & 0 \\ -\beta_z & 0 & 0 & \delta_x\bar{z}_{R,I} & 0 & -\delta_x\bar{x}_T - \phi_z \end{bmatrix} \tag{35}$$

Here, the sign of the third and the sixth rows and columns has been changed (corresponding to a sign change for variables $x_{R,I}$ and $z_{R,I}$).

We say that a system is a *strong candidate bistable system* [1, 2] if it can become unstable exclusively due to a real eigenvalue that becomes positive.

Proposition 18. *Under Assumptions 1, 2, 3, and 4, system* (27)–(32) *is a strong candidate bistable system.*

Proof. We remind that, under our assumptions, $-\kappa_z + \alpha_z z_A > 0$ and $-\kappa_x + \alpha_x x_A > 0$. Then a similarity transformation $\hat{J}_\nu = T^{-1}J_\nu T$ can be applied, with $T = \text{diag}\{-1, \ -1, \ -1, \ 1, \ 1, \ 1\}$, such that $\hat{J}_\nu$ has non–negative off–diagonal entries, namely is a Metzler matrix, and negative diagonal entries. It is known (see for instance [3]) that a Metzler matrix has a real dominant eigenvalue: in this case, this means that an eigenvalue λ_1 exists such that $Re(\lambda_i) \leq \lambda_1$, for $i = 2, 3, \ldots, 5$. Hence the proof follows. □

The bistable nature of this system can be explained as follows. The transition to instability, if it happens, is due to a real eigenvalue which crosses the origin (0), becoming positive. This implies that the determinant of the matrix changes sign. Being the overall solution bounded, this implies that other two equilibria, both locally stable, necessarily appear (see [1, 2] for details).

3.2 Analysis in the presence of direct titration reactions

3.2.1 Equilibrium conditions

To derive $\bar{z}_T$ as a function of $\bar{x}_T$, we set equations $\dot{x}_T + \dot{x}_A = 0$ and $\dot{x}_T = 0$, and we find two different expressions for $\bar{z}_{R,I}$. Equating these expressions we obtain:

$$\bar{z}_{R,I} = \frac{\alpha_x(x_T^{tot} - \bar{x}_T)\,\bar{x}_A}{\delta_x\bar{x}_T} = \frac{\kappa_x(x_A^{tot} - \bar{x}_A - \bar{x}_T)}{\delta_x\bar{x}_T + \nu_x\bar{x}_A},$$

and we find a relationship between $\bar{x}_T$ and $\bar{x}_A$ at steady state. As done before, we derive the equilibrium of $\bar{x}_A$ as the solution of the second order equation $a_x\bar{x}_A^2+b_x\bar{x}_A+c_x$, where $a_x = \left(\frac{\alpha_x\nu_x}{\delta_x}\right)\frac{x_T^{tot}-\bar{x}_T}{\bar{x}_T}$, $b_x = \left(\alpha_x(x_T^{tot}-\bar{x}_T)+\kappa_x\right)$ and $c_x = -\kappa_x(x_A^{tot}-\bar{x}_T)$. Assuming $x_A^{tot} > x_T^{tot}$, since $a_xc_x < 0$, the only admissible positive solution is:

$$\bar{x}_A(\bar{x}_T) = \frac{-b_x+\sqrt{b_x^2-4a_xc_x}}{2a_x}.$$

Finally, setting equations $\dot{x}_T+\dot{x}_A = 0$ and $\dot{z}_{R,I} = 0$ we get:

$$\bar{z}_T = \frac{\kappa_x}{\beta_z}(x_A^{tot}-\bar{x}_A(\bar{x}_T)-\bar{x}_T)+\frac{\phi_z}{\beta_z}\bar{z}_{R,I}(\bar{x}_T). \tag{36}$$

With a similar procedure we can get the equilibrium condition for $\bar{x}_T(\bar{z}_T)$ and the remaining equilibria. Once we find the admissible equilibrium values $\bar{z}_T$, $\bar{z}_A$, $\bar{x}_T$ and $\bar{x}_A$ we can find $\bar{z}_{R,I}$ and $\bar{x}_{R,I}$.

$$\begin{aligned}\dot{x}_{R,I} = 0 \quad &\Longrightarrow \quad \bar{z}_{R,I} = \frac{\kappa_x(x_A^{tot}-\bar{x}_A-\bar{x}_T)}{\delta_x\bar{x}_T+\nu_x\bar{x}_A},\\ \dot{z}_{R,I} = 0 \quad &\Longrightarrow \quad \bar{x}_{R,I} = \frac{\kappa_z(z_A^{tot}-\bar{z}_A-\bar{z}_T)}{\delta_z\bar{z}_T+\nu_z\bar{z}_A}.\end{aligned}$$

3.2.2 Structural bistability

In the presence of direct titration reactions the Jacobian becomes:

$$J_\nu = \tag{37}$$
$$\begin{bmatrix} -\alpha_z\bar{z}_A-\delta_z\bar{x}_{R,I} & \alpha_z(z_T^{tot}-\bar{z}_T) & \delta_z\bar{z}_T & 0 & 0 & 0\\ -\kappa_z+\alpha_z\bar{z}_A & -\kappa_z-\alpha_z(z_T^{tot}-\bar{z}_T)-\nu_z\bar{x}_{R,I} & \nu_z\bar{z}_A & 0 & 0 & 0\\ \delta_z\bar{x}_{R,I} & \nu_z\bar{x}_{R,I} & -\delta_z\bar{z}_T-\nu_z\bar{z}_A-\phi_x & -\beta_x & 0 & 0\\ 0 & 0 & 0 & -\alpha_x\bar{x}_A-\delta_x\bar{z}_{R,I} & \alpha_x(x_T^{tot}-\bar{x}_T) & \delta_x\bar{x}_T\\ 0 & 0 & 0 & -\kappa_x+\alpha_x\bar{x}_A & -\kappa_x-\alpha_x(x_T^{tot}-\bar{x}_T)-\nu_x\bar{z}_{R,I} & \nu_x\bar{x}_A\\ -\beta_z & 0 & 0 & \delta_x\bar{z}_{R,I} & \nu_x\bar{z}_{R,I} & -\delta_x\bar{x}_T-\nu_x\bar{x}_A-\phi_z \end{bmatrix}$$

As done earlier, the sign of the third and the sixth rows and columns has been changed (corresponding to a sign change for variables $x_{R,I}$ and $z_{R,I}$).

In the presence of direct titration reactions it is more difficult to formally show that the feedback of the two subsystems is a candidate bistable system. We can however note that:
a) For "small" ν_x and ν_z, the two subsystems are "almost" in the same condition of Proposition 18, hence bistability occurs. Also, if we can assume that $\bar{z}_A > \kappa_z/\alpha_z$ and $\bar{x}_A > \kappa_x/\alpha_x$, then the same considerations as in the case of no titration apply and a bistable behavior is expected.
b) More than one equilibrium point may appear for suitable choice of the parameters. When three equilibria appear, if the Jacobian is invertible, then necessarily one of the equilibria is unstable with a real positive unstable eigenvalues; this can be explained with the so called degree theory; we refer the reader to reference [1] for additional details. The other two equilibria are expected to be stable.
c) Numerical simulations on a wide range of parameters confirm that this system can be bistable.

3.3 Numerical simulations

3.3.1 Probability of bistable behavior

As done for the oscillator, we explored the probability of obtaining a bistable behavior for random choices of the parameters around the nominal set in Table S2. The reaction rate parameters were randomly selected in the range from 10^{-2} to 10^2 their nominal value; parameters z_T^{tot}, x_A^{tot}, x_T^{tot}, x_A^{tot} were instead varied between one tenth and

ten times their nominal value. A set of parameters is classified as bistable if a) three equilibria are identified by numerically finding the intersections of the equilibrium conditions derived earlier, and b) two of these equilibria are stable (all eigenvalues have negative real part) and one is unstable (at least one eigenvalue has positive real part). Fig. S7 and S8 show that the system can exhibit bistability in a wide range of parameters, however large titration reaction rates (Fig. S8) significantly increase the probability of bistable behavior.

Figure S7: Absence of direct titration reactions. Log plot showing the correlation between randomly chosen parameters that yield bistable behavior. Nominal parameters (Table S2) are shown in the orange diamond; reaction rate parameters were varied between a factor 10^{-2} and 10^{2} of their nominal value (with $\nu = 0$), while total concentrations were varied between one tenth and ten times their nominal value.

3.3.2 Bistable behavior in a region of the parameter space

We use parameters listed in Table S2 to explore numerically the bistability regions. As done for the randomized parameter classification, a parameter set yields a bistable behavior if three equilibria, two stable and one unstable,

Figure S8: Presence of direct titration reactions. Log plot showing the correlation between randomly chosen parameters that yield bistable behavior. Nominal parameters (Table S2) are shown in the orange diamond; parameters were varied between a factor 10^{-2} and 10^{2} of their nominal value.

Table S2: Nominal parameters for the bistable circuit

Units: [nM]	Units: [1/s]	Units: [1/M/s]
$z_T^{tot} = 100$	$\beta_z = 0.0021$	$\alpha_z = 3 \times 10^4$
$x_T^{tot} = 100$	$\beta_x = \beta_z$	$\alpha_x = \alpha_z$
$z_A^{tot} = 200$	$\kappa_z = 3 \times 10^{-4}$	$\delta_z = 3 \times 10^4$
$x_A^{tot} = 200$	$\kappa_x = \kappa_z$	$\delta_x = \delta_z$
	$\phi_z = 0.001$	$\nu_z = \delta_z$
	$\phi_x = \phi_z$	$\nu_x = \nu_z$

are identified. Here, we vary only two parameters at a time, keeping the others fixed at their nominal value. In Fig. S9 and S10 we show the bistability domains (orange regions), in the absence of direct titration reactions (Fig. S9) and in the presence of titration (Fig. S10).

In the absence of titration reactions there are many pairs of parameters where the bistability region is very narrow. This makes the system less robust over the parameter space since any change in the parameters will cause the system to lose bistability. It also shows that there is a linear correlation in many pairs of parameters for a bistable behavior: (β_z, β_x), (κ_z, κ_x), (κ_x, z_A^{tot}), (β_z, x_A^{tot}), (κ_z, x_A^{tot}), (δ_x,ϕ_z) and (δ_z, ϕ_x) show a positive correlation, while (β_z, κ_z), (β_z, z_A^{tot}), (κ_z, z_A^{tot}), (β_x, x_A^{tot}) and (κ_x, x_A^{tot}) show a negative correlation to present bistable behavior. Fig. S10 clearly shows that all the regions of bistability are expanded when the titration reaction are present.

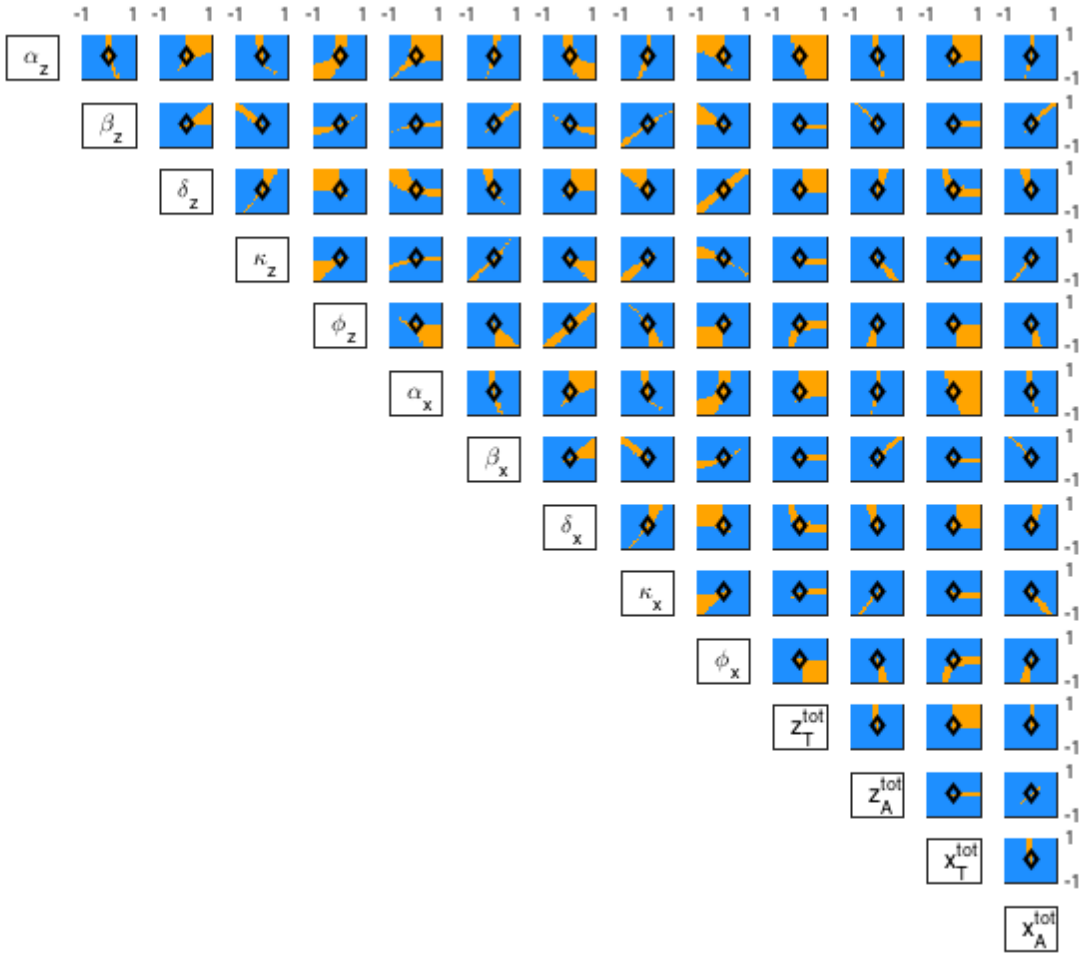

Figure S9: Absence of direct titration reactions. Axes are in log scale. The orange areas are bistable regions. Blue areas correspond to a unique stable steady state. Nominal parameters are shown as a black diamond.

Figure S10: Presence of direct titration reactions. Axes are in log scale. The orange areas are bistable regions, which are clearly expanded relative to Fig. S9. Blue areas correspond to a unique stable steady state. Nominal parameters are shown as a black diamond

References

[1] F. Blanchini, E. Franco, and G. Giordano. A structural classification of candidate oscillatory and multistationary biochemical systems. *Bulletin of Mathematical Biology*, 76(10):2542–2569, 2014.

[2] F. Blanchini, E. Franco, and G. Giordano. Structural conditions for oscillations and multistationarity in aggregate monotone systems. In *Proceedings of the 54th IEEE Conference on Decision and Control*, pages 609–614, 2015.

[3] F. Blanchini and S. Miani. *Set-theoretic methods in control*. Systems & Control: Foundations & Applications. Birkhäuser, Basel, 2015.

[4] R. Clewley, W. Sherwood, M. LaMar, and J. Guckenheimer. PyDSTool, a software environment for dynamical systems modeling. 2007.

[5] C. E. Cuba, A. R. Valle, G. Ayala-Charca, E. R. Villota, and A. M. Coronado. Influence of parameter values on the oscillation sensitivities of two p53–Mdm2 models. *Systems and Synthetic Biology*, 9(3):77–84, 2015.

[6] H. K. Khalil. *Nonlinear Systems*. Prentice Hall, 2002.